Received: 18 September 2024 | Revised: 13 December 2024 | Accepted: 30 December 2024

DOI: 10.1002/aic.18731

AIChE JOURNAL

RESEARCH ARTICLE

Process Systems Engineering

An integrated scheduling and control scheme with two economic layers for demand side management of chemical processes

Jan C. Schulze[1] | Chrysanthi Papadimitriou[1] | Paul Kolmer[1] | Alexander Mitsos[1,2,3]

[1]Process Systems Engineering (AVT.SVT), RWTH Aachen University, Aachen, Germany

[2]Energy Systems Engineering (ICE-1), Forschungszentrum Jülich GmbH, Jülich, Germany

[3]JARA-ENERGY, Jülich Aachen Research Alliance, Aachen, Germany

Correspondence
Alexander Mitsos, RWTH Aachen University, Process Systems Engineering (AVT.SVT), Aachen, Germany.
Email: amitsos@alum.mit.edu

Funding information
Bundesministerium für Bildung und Forschung, Grant/Award Number: SynErgie3; Deutsche Forschungsgemeinschaft, Grant/Award Number: 333849990/GRK2379

Abstract

Integrated dynamic scheduling (IDS) and economic nonlinear model predictive control (eNMPC) enable economic operation of chemical plants subject to volatile energy prices. Herein, we combine the two concepts into an integrated two-layer scheme. Therein, IDS performs "long-horizon" scheduling on a day-ahead (DA) market and eNMPC "short-horizon" improvements on an intra-day (ID) market. A case study demonstrates 5% economic savings over stationary operation. In contrast, stand-alone IDS and eNMPC using DA prices reach 1% and 2.5% savings, respectively. We identify arbitrage as the main driver generating the additional benefit. Additionally, we compare our scheme to stand-alone eNMPC in three ID price scenarios, where our approach consistently realizes savings of 5%. Conversely, eNMPC is price sensitive with variable revenue between 1% higher costs and 10% savings. Finally, requiring significantly shorter prediction horizons than stand-alone eNMPC, our approach eases price forecasting and enhances real-time capability.

KEYWORDS
bilevel problem, dynamic scheduling, flexible operation, hybrid model, multi-layer control

1 | INTRODUCTION

Traditionally, the two disciplines of scheduling and control have been considered as complementary but separate layers in hierarchical decision, each acting on different time scales. Over the past decades, however, the economic potential of integrating these layers has attracted a growing interest and numerous works have revealed a considerable benefit of a joint treatment.[1,2] The integration of scheduling and control is particularly advantageous in cases where the scheduling horizon comprises a significant amount of transient operation, that is, when scheduling decisions are made on the time scale of process and control dynamics.[3] Such transient operation occurs, for example, when implementing hourly or sub-hourly load changes to profit from electric energy spot markets in the context of demand response (DR) or demand-side management (DSM).[4,5] Under these circumstances, time-scale separation of the hierarchical layers is often no longer given and the de-facto interaction of the decision layers degrades economic performance when disregarded.[6,7]

Intuitively, energy-flexibilization and DSM require certain process design properties that allow for a flexible production. In this regard, flexibility capability is not only limited by the mechanical robustness of a process,[8] but also by the ability to adapt the process topology to

Both first authors contributed equally to this work.

(de)activate energy-intensive subprocesses,[9,10] store (intermediate) products,[11,12] or vary purity grades.[13] Herein, we restrict ourselves to processes that inherently provide flexibility capacities and we focus on the development of flexibility enabling operating strategies.

There are two paradigms for integrating scheduling and control, referred to as "top-down" and "bottom-up" approaches.[13] Both approaches consider the dynamics of the controlled plant in their decision making. Bottom-up strategies incorporate the scheduling task into a (usually model-based) controller by equipping the controller with an economics-driven cost function. The most prominent bottom-up approach is economic nonlinear model predictive control (eNMPC), that is, nonlinear model predictive control (NMPC) using an economic cost function.[14]

The top-down paradigm,[15,16] also referred to as integrated dynamic scheduling (IDS) hereinafter, integrates the decision layers by taking account of the open-loop or closed-loop plant dynamics in the scheduling layer. Thereby, the hierarchical architecture of process automation is preserved and the integration is addressed from the scheduling side. Various formulations of IDS have been proposed, some of which explicitly account for the closed-loop behavior due to tracking control laws by embedding the PID formula[17,18] or MPC optimality conditions.[19,20] Considering the control dynamics allows to respect (and even exploit) the joint response of process and tracking controllers in the dynamic scheduling of the production targets. Both top-down and bottom-up strategies result in optimization programs that are computationally expensive to solve. Various strategies to accelerate the solution have been proposed. These include model reduction,[11,21,22] decomposition schemes,[18,23,24] and surrogate modeling.[25–27]

Recently, we conducted a detailed comparison of the two paradigms.[28] While eNMPC promises a higher economic performance, careful controller design is needed to limit control delay due to the high computational expenses and to establish desired system properties such as stability.[29] On the other hand, IDS has the advantage of building upon an existing control infrastructure. Therein, the lower-layer stabilizing tracking controllers are usually computationally cheap and maintain the desired closed-loop properties. Clearly, irrespective of the specific implementation of the top-down paradigm, its overall performance strongly depends on the properties of the lower-layer controllers. Overall, bottom-up and top-down approaches have been considered as competing technologies for achieving the same task.[13,28,30]

Numerous studies have investigated optimal DSM of electrified chemical processes such as air separation units (ASUs)[31–33] and chlorine electrolysis.[34,35] For recent reviews see Mitsos et al. [4] and Cegla et al. .[36] Moreover, different electricity markets have been considered, in particular balancing reserve,[37,38] day-ahead (DA) auction,[39,40] and continuous intra-day (ID).[41,42] Additionally, economic benefits of simultaneously participating in multiple energy markets (particularly DA and ID markets) have attracted interest.[40,43–45] Frequently, the participation on multiple markets is considered as a two-stage problem in which the bidding proceeds in a sequential manner.[42,46]

Due to the different bidding and market clearing mechanisms, the different control paradigms are not equally suitable for the DA and ID auction and the continuous ID markets. In particular, the bidding and clearing period of the DA and ID auction markets comprise 1 h and 15 min energy products for the full next day, respectively. Hence, auction markets are particularly well suited for a day-ahead scheduling, that is, IDS. On the other hand, progressive short-term trading on a continuous ID market fits well into the eNMPC framework. Here, 15 min energy products are traded in a "pay-as-bid" fashion. However, also in a day-ahead IDS strategy, major process disturbances may trigger a re-computation of the schedule and necessitate energy purchase on the continuous ID market.

Despite a plethora of works on flexible process operation, none of the above articles on multi-market scheduling considers the dynamic effects of process control while enabling trading between different spot markets. Although there exist some strategies to combine multiple economic automation layers,[47–49] these approaches consider a single market and are rather designed for a lower-layer economic disturbance rejection. However, a strategy to harmonize multi-market participation with an integrated process control system is missing.

Herein, we combine the strengths of IDS and eNMPC into an economically superior scheme. For the computationally cheap implementation of IDS, we employ the concept of data-driven scale-bridging models.[17,25] We solve the respective IDS problem to purchase hourly energy products on the DA market in a first optimization stage. In the second stage, we employ eNMPC with a short prediction horizon to improve and exploit the scheduling decisions on the continuous ID market through real-time trading. To limit the complexity of the scheduling problem, we do not account for the (uncertain) ID market in the day-ahead scheduling computations.

We provide a literature review of the two integration approaches in Section 2 and develop an integrated automation hierarchy with two economic layers in Section 3. Section 4 introduces the ASU case study and presents the specific formulation of the scheduling problem. In Section 5, we compare the proposed scheme to the standard integrated frameworks and discuss the results. Finally, we draw conclusions in Section 6.

2 | PROCESS OPERATION SCHEMES

We briefly review the state of the art on NMPC, eNMPC, and IDS. Moreover, we discuss the concept of scale-bridging models and present Hammerstein-Wiener models as a common empirical input-output structure for scale-bridging modeling. All methods lay the foundation for the hierarchical economic scheme proposed in Section 3.

2.1 | Nonlinear model predictive control

A model predictive controller repeatedly solves an optimal control problem on a sampling grid and implements the first control move to operate the process.[50] A common formulation of the control problem reads:

$$\min_{\boldsymbol{u}} \int_{\mathcal{T}_c} \ell(\boldsymbol{x}(t),\boldsymbol{u}(t),t)\,\mathrm{d}t, \tag{1a}$$

$$\text{s.t. } M\dot{\boldsymbol{x}}(t) = \boldsymbol{f}(\boldsymbol{x}(t),\boldsymbol{u}(t)),\ \forall t \in \mathcal{T}_c, \tag{1b}$$

$$\boldsymbol{x}(t_0) = \boldsymbol{x}_0, \tag{1c}$$

$$\boldsymbol{x}(t) \in \mathcal{X},\ \boldsymbol{u}(t) \in \mathcal{U},\ \forall t \in \mathcal{T}_c, \tag{1d}$$

where $\mathcal{T}_c = [t_0, t_0 + \tau_c]$ represents the time domain with start time t_0 and prediction horizon τ_c. Further, $\boldsymbol{x}(t) \in \mathbb{R}^{n_x}$ are the states, and $\boldsymbol{u}(t) \in \mathbb{R}^{n_u}$ are the controls. The integral cost function with running cost $\ell : \mathbb{R}^{n_x} \times \mathbb{R}^{n_u} \times \mathbb{R} \to \mathbb{R}$ is minimized subject to a dynamic prediction by Equation (1b), initial conditions in Equation (1c), and admissible sets $\mathcal{X}$ and $\mathcal{U}$ of states and controls, respectively. The dynamics are represented by differential equations, wherein $\boldsymbol{f} : \mathbb{R}^{n_x} \times \mathbb{R}^{n_u} \to \mathbb{R}^{n_x}$. If the matrix $M \in \mathbb{R}^{n_x \times n_x}$ is singular, then we obtain a differential-algebraic system of equations (DAE).

The optimal control problem (1) is resolved after each sampling period Δt_s. Updating the current process states $\boldsymbol{x}_0 \in \mathbb{R}^{n_x}$ introduces feedback and is typically realized by a state estimator. Further, the controls are parameterized as piecewise constant profiles of step duration Δt_u. Depending on the formulation of ℓ, we obtain a tracking controller or an economic controller. Tracking NMPC (tNMPC) is typically realized by means of a quadratic running cost, for example:

$$\ell(\boldsymbol{x}(t)) := (\boldsymbol{x}(t) - \boldsymbol{x}_{sp})^T Q_x (\boldsymbol{x}(t) - \boldsymbol{x}_{sp}), \tag{2}$$

where Q_x is a positive semidefinite weighting matrix. Typically, the tracking setpoint $\boldsymbol{x}_{sp} \in \mathcal{X}$ is constant over the horizon (setpoint tracking NMPC), although using a reference trajectory may be advantageous in the context of flexible operation (trajectory tracking NMPC). Setpoints for the scheduling-relevant variables $\boldsymbol{v}_{sched}(t) = \boldsymbol{h}(\boldsymbol{x}(t))$, where $\boldsymbol{h} : \mathbb{R}^{n_x} \to \mathbb{R}^{n_v}$, are provided by the superior scheduling layer. For notational convenience, we use $\boldsymbol{v} = \boldsymbol{v}_{sched,sp}$ below. Then, a full vector of consistent setpoints $\boldsymbol{x}_{sp}$ is either obtained via steady-state optimization or circumvented by an adapted tracking cost function:

$$\ell(\boldsymbol{x}(t)) := (\boldsymbol{h}(\boldsymbol{x}(t)) - \boldsymbol{v})^T Q_v (\boldsymbol{h}(\boldsymbol{x}(t)) - \boldsymbol{v}), \tag{3}$$

where $Q_v \in \mathbb{R}^{n_v \times n_v}$ is again positive semidefinite. Additional terminal cost and constraints can be added to Equation (1) to establish recursive feasibility and stability.[51]

Economic NMPC is obtained when specifying an economic cost function, for example:

$$\ell(\boldsymbol{x}(t),\boldsymbol{u}(t),t) := P(\boldsymbol{x}(t),\boldsymbol{u}(t)) \cdot \mathcal{C}^e(t), \tag{4}$$

where P represents the power demand at a given operating point and $\mathcal{C}^e(t)$ is the variable energy price. Further, economic constraints can be included in Equation (1). Again, additional cost terms or constraints may be added to the control problem to establish properties such as stability.[14,29]

2.2 | Integrated scheduling and real-time optimization concepts

There are four strategies to realize the top-down paradigm for continuous processes. In the literature, these strategies have been adopted to both scheduling and real-time optimization (RTO) tasks. As we only consider single-product plants here, we do not distinguish between scheduling and RTO. Below, we provide a brief review of the strategies.

2.2.1 | Transition tables

The first class of integration approaches equips the steady-state scheduling model with dynamic ramping constraints to account for the transition times between operating points.[32,52–56] Due to the quasi-stationary modeling, the scheduling problem remains relatively simple, and the pre-computation of "transition tables" can be decoupled from the scheduling calculations.[57] However, the approach relies on simple, for example, linear, transition profiles and completed transitions between well-defined steady states. Both requirements pose a considerable restriction to processes with distinct transients.

2.2.2 | Open-loop dynamic optimization

In order to rigorously account for the transient process behavior, the optimization can be formulated as a dynamic scheduling or dynamic real-time optimization (DRTO) problem, employing a mechanistic multi-time-scale process model.[58,59] In the context of DSM, the approach was later adapted by several authors.[3,5,11,60,61] Solving this *open-loop* problem provides the reference trajectories for state and controls to the lower-layer tracking controller, cf. Equation (2). However, this type of scheduling problem still represents a very idealized perspective, where the *closed-loop* effects due to the tracking control laws, plant-model mismatch, disturbances, and other factors are disregarded. In addition, the optimal schedule is relatively expensive to (re-)compute. To address the computational aspect, low-order reduced models may be constructed to capture only the scheduling-relevant dynamics in the open-loop DRTO problem.[6,42,62]

2.2.3 | Closed-loop dynamic optimization

A tighter integration of the layers is achieved by embedding the control laws as additional constraints into the DRTO problem, for example, including the PID formula[18] or lower-layer MPC algorithm.[19,20,63,64] Thereby, the dynamic closed-loop (setpoint-to-output) process behavior is explicitly accounted for in the scheduling computations. Since the transient operating phases and associated control moves are captured more realistically, this approach provides superior schedules.[19,20,42] Kumar et al. [65] observed an analogue effect for the integration of base layer control and supervisory control, where modeling the PID base

layer dynamics in an MPC prediction model improved the overall closed-loop performance in some cases.

From a system-theoretic perspective, embedding the (closed-loop) tracking control law into the DRTO problem is the most rigorous approach to layer integration. However, embedding an MPC algorithm, that is, a sequence of MPC optimization problems, into the scheduling program leads to highly complex bilevel programs. Such scheduling programs are typically nonconvex and non-differentiable due to complementarity constraints arising from the Karush-Kuhn-Tucker conditions of constrained MPC problems. Despite first results on input-constrained MPC,[20,66,67] accounting for the closed-loop behavior of output-constrained MPC remains an open research problem towards the application of lower-level MPC. Moreover, disturbing effects such as plant-model mismatch are difficult to capture by this approach. At the same time, most of the information contained in the lower-level problem is not relevant to the scheduling decision making.[25]

2.2.4 | Low-order closed-loop dynamic optimization

The computational burden described in Section 2.2.3 can be lowered by substituting the representation of the process under supervisory tracking control by a reduced input-output model of the closed-loop process response.[17,25,68] Such low-order representations are termed "scale-bridging models" (SBMs) and encapsulate the feedback structure of control law and dynamic plant response as visualized in Figure 1. Another variant of this approach was presented by Du et al. ,[69] who parameterized the reference trajectory by a dynamic model rather than capturing the closed-loop process response. We regard their approach as a hybrid version of transition tables and SBMs.

SBMs can be obtained through model reduction,[69] empirical model identification from closed-loop simulations,[25] or techniques to approximate the lower-level problem from the previous paragraph.[64] Data-driven SBMs can also be directly identified using historical operating data from the plant.[70] This last case does not require a detailed plant surrogate and is inherently capable to account for plant-model mismatch of a model-based controller. Finally, an SBM may be built as a combination of mechanistic and data-driven submodels, that is, a hybrid model (further details in Section 2.3).

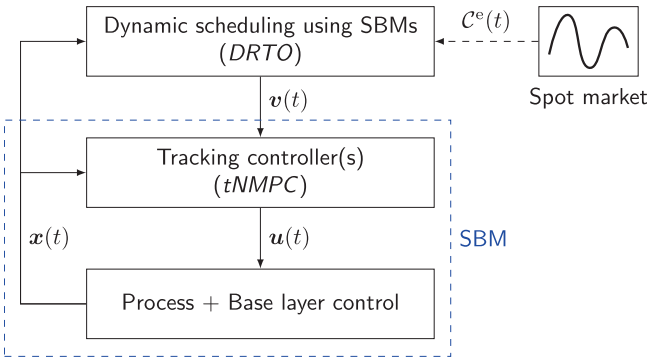

FIGURE 1 Integrated scheduling and control using scale-bridging models (SBMs).

SBM-based IDS may be able to compensate poor tracking behavior to some extend, yet we cannot expect an overall high performance in such cases. On the other hand, SBMs require updating if the scheduling-relevant dynamics are altered, for example, through changes made on the controller tuning. Further, the complexity of SBM identification grows with the number of setpoint parameters, for example, when using multiple setpoints or reference trajectories.

Closed-loop dynamic scheduling has been used extensively in the recent literature and typically achieve economic savings between 1% and 15% on day ahead market compared to stationary operation.[25,28,67,71] In extreme cases, savings up to 50% have been reported.[19,72] We remark that cost savings strongly depend on the chosen benchmark case and the price profile. Hence, a too conservative benchmark operating point may suggest higher than realistic savings due to a high power consumption reference.

In most works on IDS, tracking controllers without output constraints have been considered, which are characterized by a sufficiently smooth closed-loop setpoint-tracking response.[25] Conversely, in the presence of hard output constraints, the closed-loop response can be non-smooth and smooth SBMs are at best moderately accurate. This observation is consistent with the discussion in Section 2.2.3 and references cited therein. To improve the overall constraint satisfaction, strict output (hard) constraints may be formulated at the scheduling level. These (back-off) constraints are more conservative than the controller constraints.[70,73] Similar to control law embedding, the identification of non-smooth SBM for processes under output-constrained (N)MPC remains an open research problem. Consequently, we herein limit ourselves to input-constrained tracking NMPC.

2.3 | Scale-bridging models

We consider IDS using SBM as a practical compromise of complexity and accuracy of the computations. Recall that an SBM describes the dynamic response of the scheduling-relevant process variables $\boldsymbol{y}$ to changes in the scheduling degrees of freedom $\boldsymbol{v}$, that is, the setpoints to the tracking controllers. For example, $\boldsymbol{y}$ may contain both the energy consumption and the production rate. To formulate the respective scheduling problem, we denote a generic SBM by:

$$\mathbf{0} = \boldsymbol{f}^{\mathrm{SBM}}(\boldsymbol{z}(t), \dot{\boldsymbol{z}}(t), \boldsymbol{y}(t), \boldsymbol{v}(t)), \tag{5}$$

where $\boldsymbol{z}(t)$ are differential (data-driven) states of the SBM. Notice that we may alternatively use a discrete-time model, for example, an autoregressive model.[71] Herein, we consider a hybrid SBM combining mechanistic and data-driven scale-briding submodels. In particular, we employ mechanstic dynamic models of the scheduling-relevant product storage tanks. On the other hand, the main production process is captured by data-driven SBMs. Combing the submodels by means of

complementary energy and mass balances yields an overall hybrid SBM.

Different types of data-driven SBMs have been used in the literature, including linear[17,68,69] and block-structured[25,74] models. Hammerstein-Wiener (HW) models represent a good compromise between a simple structure and reliable long-term forecasts.[75] In addition, strategies to exploit the nonlinear HW block structure in dynamic optimization are known.[74,76,77] Consequently, we adopt Hammerstein-Wiener models as data-driven SBMs here. Single-input single-output (SISO) HW models can be stated in continuous-time state-space representation as follows:

$$\dot{\boldsymbol{z}}(t) = \mathbf{A}\boldsymbol{z}(t) + \mathbf{B} f_{\mathrm{H}}(v(t)),\ \boldsymbol{z}(0) = \mathbf{0}, \tag{6a}$$

$$y(t) = f_{\mathrm{W}}(\mathbf{C}\boldsymbol{z}(t) + \mathbf{D} f_{\mathrm{H}}(v(t))), \tag{6b}$$

where $v(t) \in \mathbb{R}$ is the single SBM input (i.e., subprocess control setpoint), $f_{\mathrm{H}} : \mathbb{R} \to \mathbb{R}$ is the nonlinear (Hammerstein) input map, and $f_{\mathrm{W}} : \mathbb{R} \to \mathbb{R}$ is the nonlinear (Wiener) output map. Different function types can be used for the nonlinear blocks, such as piecewise linear, polynomials, sigmoid networks, and ANNs.[28,75,77] Further, $\mathbf{A} \in \mathbb{R}^{n \times n}$, $\mathbf{B} \in \mathbb{R}^{n \times 1}$, $\mathbf{C} \in \mathbb{R}^{1 \times n}$, and $\mathbf{D} \in \mathbb{R}^{1 \times 1}$ are linear system matrices. In the case of multiple scheduling-relevant variables y_i, several SISO models are used. HW models can be identified from recorded plant data or closed-loop simulation records through a system identification toolbox, for example, MATLAB.

2.4 | Formulation of dynamic scheduling problem using SBM

The generic form of the IDS-DRTO scheduling problem with SBM embedded reads:

$$\begin{aligned} \min_{\boldsymbol{v}(t) \in \mathcal{V}} \ & \int_{\mathcal{T}_{\mathrm{s}}} P(t) \cdot \mathcal{C}^{\mathrm{e}}(t)\, \mathrm{d}t \\ \text{s.t. } \mathbf{0} &= \boldsymbol{f}^{\mathrm{SBM}}(\boldsymbol{z}(t), \dot{\boldsymbol{z}}(t), \boldsymbol{y}(t), \boldsymbol{v}(t)), P(t) = y_1(t), \\ \mathbf{0} &\geq \boldsymbol{c}(\boldsymbol{y}(t), \mathcal{C}^{\mathrm{e}}(t), t),\ t \in \mathcal{T}_{\mathrm{s}}. \end{aligned} \tag{7}$$

Therein, $\mathcal{T}_{\mathrm{s}} = [0, \tau_{\mathrm{s}}]$ is the scheduling time domain and $\boldsymbol{v} : \mathcal{T}_{\mathrm{s}} \to \mathbb{R}$ are the scheduling degrees of freedom, for example, controller setpoints. We assume a piecewise constant parameterization of $\boldsymbol{v}$ in an admissible set $\mathcal{V}$. The running cost is similar to Equation (4) but additional cost terms may be added. The power demand $P(t)$ is assumed to be the first output of the scale-bridging model and $\mathcal{C}^{\mathrm{e}}(t)$ is the electricity price. Finally, $\boldsymbol{c}$ is a generic map to represent path and point constraints.

Solving the IDS problem (7) provides optimal controller setpoints $\boldsymbol{v}^{\star}(t)$. Since we focus on scheduling for DSM of continuous single-product plants, we do not consider multi-product scheduling,[70,78] variable product grade, or flexible production order.[79] Furthermore, while the scheduling problem involves a sequence of setpoints, these are only successively given to the controllers, that is, the lower-layer controllers are setpoint tracking controllers given a single setpoint, $\boldsymbol{v}^{\star}(t)$, rather than reference trajectory tracking controllers. The extension of the proposed method by these aspects is left for future investigations.

Irrespective of the type of tracking controller, some of the operating constraints may be economically critical and should therefore be incorporated as scheduling constraints. One common example is product quality, where on the one hand over-purification curtails economic benefit and on the other hand quality violations (under-purification) result in production losses.[80] Adding such economically critical quantities as scheduling constraints or even setpoints may hence enable an extra economic profit.

3 | TWO-LAYER SCHEDULING AND ENMPC SCHEME

As previously discussed, the competing paradigms IDS and eNMPC are practically most suited for different types of energy markets. Hence, we propose to combine the two strategies into an integrated two-economic-layers (TEL) scheme. We introduce the basic concept in Section 3.1 and provide a mathematical formulation in Section 3.2.

3.1 | Basic concept

The TEL strategy combines the top-down and bottom-up paradigms and is visualized by Figure 2. In the top economic layer, we employ IDS to participate in an auction market. To keep the scheduling problem simple, we do not include the uncertain continuous ID market at this stage but perform a pure DA scheduling. In the subordinate economic layer, eNMPC is used for process control and for short-term economic improvements on a continuous trading market, that is, continuous ID market.

The automation layers are integrated as follows. Similar to standalone IDS, the top-layer scheduling employs an SBM of the process under supervisory (economic) control. However, as we do not consider the ID market at this stage, the economic controller(s), here

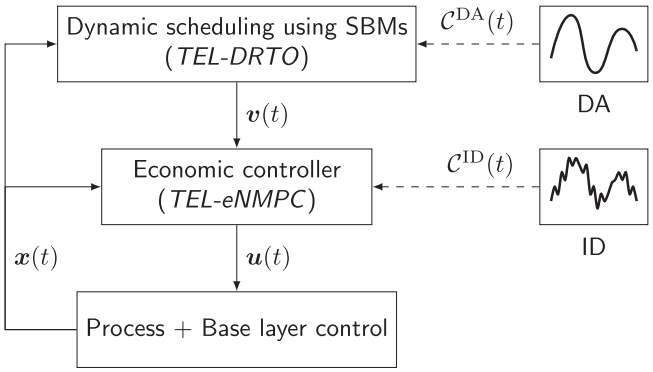

FIGURE 2 Proposed TEL scheme for integrated scheduling and control with electricity arbitrage.

eNMPC, acts as an energy tracking controller with no degrees of freedom for economic optimization. Solving the IDS provides a power consumption reference and process variables schedule to the eNMPC. The eNMPC optimizes a prediction model of the process and base-layer controllers.[65] Given the IDS power reference, the eNMPC generates further economic profit by performing real-time economic corrections through trading on a continuous market, here ID market. These improvements are absent a conventional top-down approach, where tracking controllers realize process operation according to the schedule. In contrast, TEL-eNMPC is able to exploit short-term fluctuations in the energy price over the prediction horizon by purchasing or offering energy volumes. This mechanism is called arbitrage and further discussed in the case study below.

Intuitively, economic improvements from such a TEL strategy will grow with increasing differences in the prices on the two markets, as long as temporal price deviations occur in both directions, that is, we can switch between buying and selling energy products. Thereby, an additional economic benefit over classic IDS is realized through arbitrage. An approximately zero-mean difference between DA and ID prices, that is, a balanced positive and negative deviation, is very common and thus a legitimate assumption.[81] Based on the procedure and frequency of DA market clearing, for example, every 24 h on EPEX Spot market, the IDS calculations are performed rather infrequently. Conversely, eNMPC optimizations are executed recursively at the controller frequency, for example, seconds to minutes. Here, the process state as well as the ID prices are updated at every sampling point.

An important property of the TEL structure is that the eNMPC prediction horizon can be relatively short compared to a stand-alone eNMPC application. Specifically, the prediction horizon only needs to be long enough to control the process and contain a sufficient amount of positive and negative deviation of the ID price from the DA price to benefit from market deviations. As discussed by Germscheid et al. [45] and Papadimitriou et al. ,[81] the principal frequencies of such market deviations are in the range of $0.5\,\mathrm{h}^{-1}$ to $2\,\mathrm{h}^{-1}$. Hence, we can expect that short eNMPC horizons spanning a few hours are sufficient, which is a major advantage of our TEL strategy. In particular, the long prediction horizons needed in stand-alone eNMPC implementation constitute a major computational obstacle to practical eNMPC applications.[82]

3.2 | Mathematical formulation

The task is a two-stage optimization problem with each stage corresponding to an economic layer. At the first stage (top layer), we compute an optimal schedule by solving Equation (7). Therein, the SBM encapsulates the closed-loop dynamic response of the process and economic controller. We only consider DA spot market at the first stage and assume that $\mathcal{C}^{\mathrm{DA}}$ is known.

The key observation for constructing a corresponding SBM is that an economic controller behaves like a tracking controller when restricted to a fixed power and production schedule with no freedom for economic decision making. This observation simplifies the closed-loop data collection and SBM identification considerably. In fact, we may simplify the problem further by embedding the SBM of a setpoint tracking controller into the IDS problem, provided that the optimal values $\boldsymbol{v}^{\star}(t)$ constitute a feasible reference for the economic controller in the lower layer. For example, this requirement is fulfilled for setpoint tracking NMPC and eNMPC with identical setup except for the cost function. Since an SBM of setpoint tracking NMPC is easier to obtain, we pursue this strategy here.

At the second stage, we repeatedly solve an eNMPC problem in closed-loop operation. Here, the eNMPC can operate the process more freely than tNMPC by purchasing additional energy on the ID market and no strict ASU production schedule. Only a reference profile of already purchased energy is provided by the upper scheduling layer. However, we must include additional requirements and economic constraints to the eNMPC problem, going beyond a tNMPC formulation. In particular, to fulfill the power consumption commitment, the hourly DA energy products must be consumed by the process or sold on the ID market. Further examples of economic constraints include: i) limits on the amount of energy traded on the continuous market, ii) endpoint constraints on the eNMPC prediction horizon (e.g., total production or quality as scheduled), and iii) fixed time point constraints (e.g., an end-of-the-day constraint on the process inventories).

We formulate the eNMPC optimization problem as a variant of Equation (1) by specifying the economic stage cost:

$$\ell(\boldsymbol{x}(t),\boldsymbol{u}(t),t) = \Delta P(\boldsymbol{x}(t),\boldsymbol{u}(t),t)\cdot\mathcal{C}^{\mathrm{ID}}(t). \tag{8}$$

Therein, $\mathcal{C}^{\mathrm{ID}}$ is the energy price on the continuous ID market and ΔP describes the deviation of energy consumption from the IDS schedule, that is, $\Delta P(\boldsymbol{x}(t),\boldsymbol{u}(t),t) = P(\boldsymbol{x}(t),\boldsymbol{u}(t)) - P^{\mathrm{IDS}}(t)$, where $P^{\mathrm{IDS}}(t)$ is the process power consumption as scheduled and purchased due to IDS. Since IDS considers DA prices, we use $P^{\mathrm{IDS}}(t)$ and $P^{\mathrm{DA}}(t)$ interchangeably. The deviation $\Delta P(t)$ reflects the power purchased ($\Delta P(t) > 0$) or sold ($\Delta P(t) < 0$) on the ID market, wherefore $P^{\mathrm{ID}}(t) = \Delta P(t)$. Hence, for $P^{\mathrm{ID}} \equiv 0$ the IDS schedule is tracked exactly, that is, eNMPC acts as a "power tracking controller".

4 | CASE STUDY

We assess the performance of the TEL operating strategy on the nitrogen-product ASU with product storage from Caspari et al. ,[28] shown in Figure 3. The ASU is composed of the main air compressor (MAC), two plate-fin multi-stream heat exchangers (PHX1, PHX2), two turbines (TURB1, TURB2), a high-pressure distillation column (HPC) with heat-integrated reboiler and condenser (IRC). The product storage system includes a liquefaction unit, a storage tank, and an evaporator.

The scheduling-relevant variables (SRVs) for IDS and eNMPC are the ASU production rate F_{asu}, the molar fraction of impurities in the product l_{asu}, the product demand F_{dem}, the power intake of the main

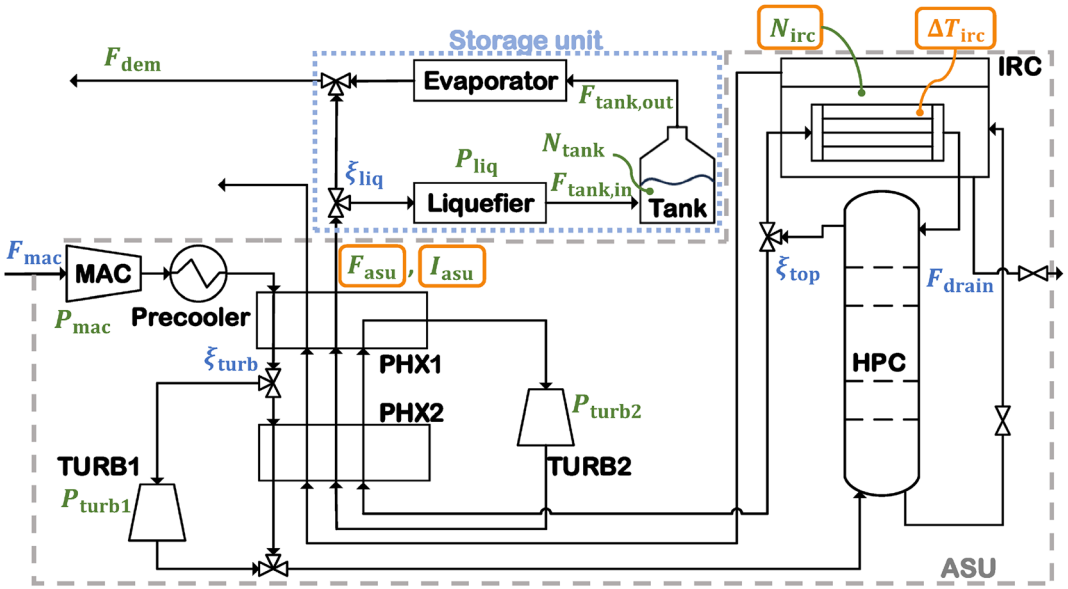

FIGURE 3 Schematic representation of the ASU, adapted from Caspari et al. .[28] MVs in blue, SRVs in green, and CVs framed in orange.

compressor P_{mac}, and the power output of the two turbines P_{turb1} and P_{turb2}. Moreover, the power consumption of the liquefier P_{liq} and the input and output flow rates of the storage tank $F_{tank,in}$ and $F_{tank,out}$ are SRVs. The temperature difference ΔT_{irc} between reboiled and condensed medium in the IRC is control relevant but not scheduling relevant as we discuss below. Finally, the tank levels of reboiler N_{irc} and storage unit N_{tank} have integrating behavior and must therefore be controlled, with N_{tank} also being scheduling relevant.

The control inputs of the process are the molar flow rate of the feed air stream F_{mac}, the split fraction ξ_{turb} of air flow into the turbine, the split fraction ξ_{liq} of the product stream into the liquefier, the reflux fraction ξ_{top}, and the liquid drain from the reboiler F_{drain}. The product demand F_{dem} is met by mixing gaseous product from the ASU and evaporated product from the storage tank. We do not consider the product storage system as part of the ASU. Instead, we treat the ASU and storage system as two connected subsystems. While IDS and economic NMPC optimize the total system, tracking NMPC only deals with the ASU subsystem.

In nominal operation, the ASU produces 20 mol/s nitrogen product at 1500 ppm impurity content. The corresponding power demand is $P_{asu} = 296.8$ kW. Further, the process inventories are $N_{irc} = 25$ kmol and $N_{tank} = 1728$ kmol and defined as 100%. The nominal storage tank holdup corresponds to a full-day production volume. We assume that the process is initially at its nominal operating point.

4.1 | Implementation

The scheduling and control framework is implemented in Python 3.6 and employs our open-source dynamic optimization framework DyOS.[9] Therein, DyOS combines the DAE integrator NIXE[83] and NLP solver SNOPT.[84] We specify an optimality tolerance of `1E-4`, feasibility tolerance of `1E-3`, and integration tolerances of `1E-5`. The full-order model and SBMs are written in Modelica and accessed through a Functional Mock-up Interface. All computations are executed on a server with Intel®Xeon®E5-2640 v3 CPU @ 2.60 with 128 GB RAM.

4.2 | Top-down IDS

The degrees of freedom in the IDS problem are the manipulated variables of the storage system as well as the ASU production rate setpoints $F_{asu,sp}$ transmitted to the tNMPC. Before formulating the IDS problem, we present the tNMPC setup and the resulting SBM.

4.2.1 | Tracking NMPC

We formulate the tNMPC based on Equation (1) using the full-order dynamic model of the ASU subsystem in combination with quadratic tracking cost:

$$\begin{aligned}\ell(\cdot) &= \omega_1 \cdot (F_{asu}(t) - F_{asu,sp})^2 + \omega_2 \cdot (I_{asu}(t) - I_{asu,sp})^2 \\ &\quad + \omega_3 \cdot (\Delta T_{irc}(t) - \Delta T_{irc,sp})^2 + \omega_4 \cdot (N_{irc}(t) - N_{irc,sp})^2,\end{aligned} \tag{9}$$

where ω_i are constant weights and the constant setpoints of the controlled variables (CVs) are indicated by "sp". The production rate setpoint $F_{asu,sp}$ may change between tNMPC optimizations, whereas the other setpoints are generally fixed. The manipulated variables (MVs) are $\boldsymbol{u} = [F_{mac}, \xi_{turb}, \xi_{top}, F_{drain}]^T$. We employ piecewise constant controls of $\Delta t_u = 5 textmin$ duration and do not penalize the magnitude of step changes. Table 1 collects the tNMPC weights, setpoints, and input constraints. To enable flexible operation rather than (inflexible)

TABLE 1 Controller tuning of tNMPC.

Variable	Unit	Type	Weight (ω_i)	Values (SP or MV)
F_{asu}	mol/s	CV	1.0	[15,25]
l_{asu}	ppm	CV	0.003	10
ΔT_{irc}	K	CV	10^{-5}	2.5
N_{irc}	%	CV	10^{-4}	100
F_{mac}	mol/s	MV	–	[30,55]
F_{drain}	mol/s	MV	–	[0,2]
ξ_{turb}	–	MV	–	[0,0.1]
ξ_{top}	–	MV	–	[0.51,0.54]

constraint tracking, the impurity setpoint of 1000 ppm is below the maximum 1500 ppm.

We do not impose any state or output constraints because such constraints can result in a nonsmooth closed-loop response and thus prohibit the application of HW SBMs. Including such constraints will require further research within future works. Finally, process feedback is realized by means of full state feedback.

4.2.2 | SBM identification

We generate an identification data set comprising the response of the SRVs of the ASU under tNMPC to step changes in the production rate setpoint $F_{asu,sp}$. To this end, we initialize the ASU at 1000 ppm product quality and generate a random sequence of setpoints, $F_{asu,sp} \in [15,25]$, on a 72 h horizon. The training data set combines slow and fast setpoint step changes of 3.75 and 0.25 h duration, respectively, to account for both slow and fast process dynamics. In a similar fashion, we construct a test data set of 10 h duration, comprising 1 and 0.25 h steps in the production setpoint.

The ASU production rate F_{asu} as well as the ASU power demand P_{asu} are both SRVs. Furthermore, an investigation of the identification data set reveals that the product impurity l_{asu} temporarily exceeds the targeted impurity limit of 1500 ppm. Recall that our tracking NMPC is merely input-constrained, wherefore such a high impurity is not infeasible from the NMPC perspective. However, due to quality requirements, the product impurity is scheduling-relevant and will be hard-constrained in the scheduling problem. Since all other CVs of tNMPC do not exceed the operating limits in the identification data set, we assume that these are uncritical and not scheduling relevant.

We scale the training data to the value range $[0,1]$ and use the MATLAB 2023 System Identification Toolbox to generate HW models for all SRVs. For the model selection, we perform training over a wide selection of hyperparameters (e.g., type of nonlinearities, order of linear dynamics) and select the model with the lowest normalized Akaike criterion (nAIC), similar to.[75] The types of nonlinearities examined are polynomials, sigmoid networks, ANNs, DNNs with the hyperbolic tangent and sigmoid activation functions. After training, the resulting model is validated on the test data set. The resulting models use polynomials (F_{asu}, l_{asu}) and ANNs (P_{asu}) for the nonlinear blocks, and fifth to eighth order of linear dynamic blocks. Table 2 lists the train and test accuracy of the models in terms of the normalized root mean squared error (NRMSE). The values are comparable to Pattison et al. [25] and Tsay et al. .[70]

TABLE 2 SBM identification results.

Variable	Train fit	Test fit
F_{asu}	99.65%	99.56%
P_{asu}	91.04%	89.19%
l_{asu}	71.90%	85.62%

Figure 4 depicts model testing for the impurity and power prediction. Therein, the transients of the closed-loop response to tNMPC setpoint changes are clearly visible, supporting the application of a dynamic SBM. Despite some deviations, both SBMs capture the major dynamic trends. Detailed information on the identification is provided in the SI.

4.2.3 | IDS problem formulation

Combining the SMBs with a mechanistic model of the product storage systems results in a hybrid process model and the upper-layer IDS-DRTO problem (7) becomes:

$$\min_{F_{asu,sp},\,\xi_{liq}} \int_{\mathcal{T}_s} \left(P_{asu}(t)+P_{liq}(t)\right)\cdot \mathcal{C}^{DA}(t)\,\mathrm{d}t, \tag{10a}$$

$$\text{s.t. } F_{asu}(t) = f_{HW,1}(t,F_{asu,sp}), \tag{10b}$$

$$P_{asu}(t) = f_{HW,2}(t,F_{asu,sp}), \tag{10c}$$

$$l_{asu}(t) = f_{HW,3}(t,F_{asu,sp}), \tag{10d}$$

$$\dot{N}_{tank}(t) = F_{tank,in}(t)-F_{tank,out}(t), \tag{10e}$$

$$F_{tank,in}(t) = \xi_{liq}(t)\cdot F_{asu}(t), \tag{10f}$$

$$P_{liq}(t) = f_{liq}\left(\xi_{liq}(t)\cdot F_{asu}(t)\right), \tag{10g}$$

$$F_{dem}(t) = (1-\xi_{liq}(t))\cdot F_{asu}(t)+F_{tank,out}(t), \tag{10h}$$

$$\boldsymbol{v}(t) \in \mathcal{V}, \boldsymbol{y}(t)\in\mathcal{Y}(t), \boldsymbol{z}(t)\in\mathcal{Z}(t), \tag{10i}$$

where $\tau_s = 24$ h. Equations (10b) to (10d) are the data-driven SBMs initialized at the nominal operating point, Equations (10e) to (10g) describe the storage system, and the path equality constraint in Equation (10h) determines $F_{tank,out}$ and ensures that the product demand is met. Equation (10i) represents the path and endpoint

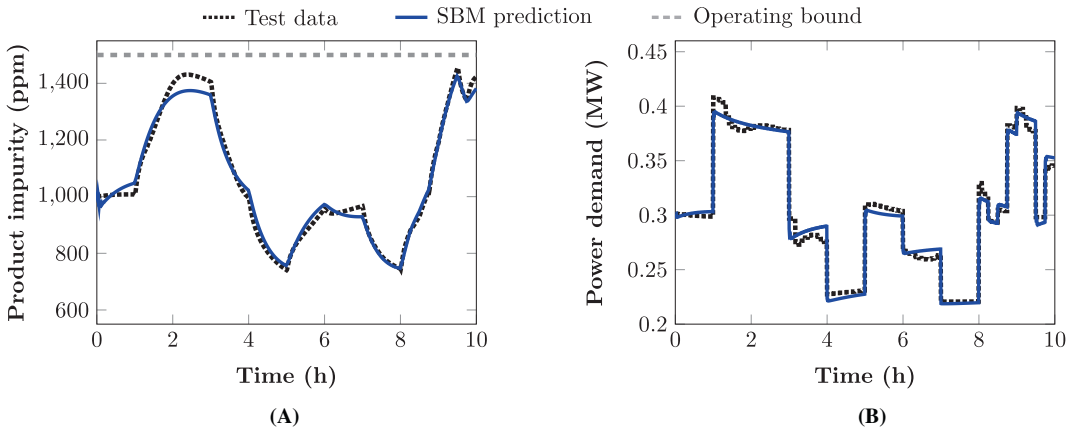

FIGURE 4 Testing of the identified SBMs. (a) Product impurity, (b) ASU power demand.

TABLE 3 Constraints in IDS-DRTO problem.

Variable	Unit	Value set	Time set
I_{asu}	ppm	[0,1500]	$\mathcal{T}_s$
$F_{tank,in}$	mol/s	[0, 10]	$\mathcal{T}_s$
$F_{tank,out}$	mol/s	[0, 10]	$\mathcal{T}_s$
N_{tank}	%	[0, 200]	$\mathcal{T}_s$
N_{tank}	%	{100}	$\{\tau_s\}$
$F_{asu,sp}$	mol/s	[15, 25]	$\mathcal{T}_s$
ξ_{liq}	–	[0, 1]	$\mathcal{T}_s$

constraints as detailed in Table 3. The periodic endpoint constraint on N_{tank} guarantees that the storage tank is only used to balance temporal over- and underproduction but not systematically drained over a day.

The two scheduling variables, $\boldsymbol{v} = [F_{asu,sp}, \xi_{liq}]^T$, are parameterized as piecewise constant functions of fixed step length. Preliminary experimentation with the value grid of $F_{asu,sp}$ suggested that 1 h intervals are a suitable choice, matching with the 1 h energy products on the DA market. On the other hand, 20 min intervals are used for ξ_{liq}.

4.3 | Bottom-up eNMPC

The stand-alone eNMPC uses a full-order model of the total process (ASU + storage system) and an economic cost similar to Equation (10a), where the running cost:

$$\ell(\cdot) = (P_{asu}(t) + P_{liq}(t)) \cdot \mathcal{C}^e(t). \tag{11}$$

Since the DA market clearing and eNMPC time horizon generally do not harmonize, an eNMPC based on DA prices, $\mathcal{C}^e(t) = \mathcal{C}^{DA}(t)$, is purely hypothetical and only considered for comparison. Besides this hypothetical benchmark, we use continuous ID prices $\mathcal{C}^{ID}(t)$, being a more realistic scenario for stand-alone eNMPC.

TABLE 4 Input and state constraints in eNMPC problem. Current time t_0 and prediction horizon τ_c determine the prediction time domain $\mathcal{T}_c = [t_0, t_0 + \tau_c]$

Variable	Unit	Type	Value set	Time set
F_{asu}	mol/s	CV	[15, 25]	$\mathcal{T}_c$
I_{asu}	ppm	CV	[0,1500]	$\mathcal{T}_c$
ΔT_{irc}	K	CV	[1,5]	$\mathcal{T}_c$
N_{irc}	%	CV	[20,160]	$\mathcal{T}_c$
N_{irc}	%	CV	{100}	$\{t_0 + \tau_c, 24\,h\}$
$F_{tank,in}$	mol/s	CV	[0, 10]	$\mathcal{T}_c$
$F_{tank,out}$	mol/s	CV	[0, 10]	$\mathcal{T}_c$
N_{tank}	%	CV	[0, 200]	$\mathcal{T}_c$
N_{tank}	%	CV	{100}	$\{t_0 + \tau_c, 24\,h\}$
F_{mac}	mol/s	MV	[30, 55]	$\mathcal{T}_c$
F_{drain}	mol/s	MV	[0, 2]	$\mathcal{T}_c$
ξ_{turb}	–	MV	[0, 0.1]	$\mathcal{T}_c$
ξ_{top}	–	MV	[0.51, 0.54]	$\mathcal{T}_c$
ξ_{liq}	–	MV	[0, 1]	$\mathcal{T}_c$

The MVs include all control inputs of the process, that is, F_{mac}, ξ_{turb}, ξ_{top}, F_{drain}, and ξ_{liq}. The CVs comprise all economically and control-relevant variables, see Table 4. We formulate path and point constraints on the MVs and CVs and provide the respective sets in Table 4. In particular, we formulate prediction horizon endpoint constraints on the tank inventories to recover the nominal values. This endpoint constraint ensures recursive feasibility of the control program. Additionally, we include end-of-the-day point constraints on the tank inventories to prevent tank draining. Besides optimizing more degrees of freedom than tNMPC and IDS-DRTO, the eNMPC problem also involves the larger number of constraints. The sampling time is $\Delta t_s = 5$ min in all cases. Further, we implement full state feedback.

4.4 | Two-layer IDS and eNMPC

We implement the TEL scheme as described in Section 3. Since we employ the SBM under tracking NMPC, the upper-layer scheduling problem (TEL-DRTO) is identical to Equation (10). Solving the TEL-eNMPC problem yields the scheduled power consumption $P^{\mathrm{DA}}(t) = P^{\mathrm{DA}}_{\mathrm{asu}}(t) + P^{\mathrm{DA}}_{\mathrm{liq}}(t)$. The lower-layer eNMPC (TEL-eNMPC) is an extended version of the stand-alone eNMPC described in the previous section. Specifically, we use the economic running cost:

$$\ell(\cdot) = P^{\mathrm{DA}}(t) \cdot C^{\mathrm{e}}_{\mathrm{DA}}(t) + \Delta P(t) \cdot C^{\mathrm{e}}_{\mathrm{ID}}(t), \tag{12}$$

where $\Delta P(t) = P_{\mathrm{asu}}(t) + P_{\mathrm{liq}}(t) - P^{\mathrm{DA}}_{\mathrm{asu}}(t) - P^{\mathrm{DA}}_{\mathrm{liq}}(t)$ captures the deviation from the power schedule. Further, we modify the constraints on the storage tank level N_{tank} as stated by Table 5. Constraint (iii) ensures that TEL-eNMPC optimizes around the scheduled reference, $N^{\mathrm{DA}}_{\mathrm{tank}}(t)$, instead of targeting the nominal level at the end of each eNMPC optimization.

4.5 | Definition of operating scenarios

We compare the proposed TEL strategy to the single-layer eNMPC and IDS approaches. Besides evaluating the economic revenue, we contrast the operating strategies with respect to practical aspects. Specifically, we examine different tNMPC and eNMPC prediction horizons ranging from 2 to 12 h for all methods.

As a base case and benchmark, we consider nominal steady-state operation of the ASU subject to DA and ID prices. This nominal operating point is the optimal steady state with minimum power demand at 20 mol/s production rate at 1500 ppm purity grade. We consider a scheduling horizon of 24 h length and hence use single-day DA and ID price profiles. To avoid issues with a shrinking horizon at the end of the day, we define a periodic scenario, that is, all prices repeat after 24 h.

We use the DA and ID price scenarios from our recent publication.[81] To represent the ID price, we select the ID_3 index, which is the volume-weighted average price of all trades that took place within the last three hours before delivery.[85]

The DA and ID price scenarios comprise 24 h and are constructed based on historical data of European spot markets. The DA and ID profiles are constructed through an averaging scheme, which includes an ID baseline correction to ensure that the 24 h cumulative price difference between DA and ID profiles is zero-mean distributed.[81] Aligning the ID and DA profiles in this way improves comparability and generalizability of the results. The resulting price scenario is shown in Figure 5 and additionally provided via Git.*

In addition to this first case, we consider two price scenarios with non-matching mean price of the DA and ID profiles. Here, the ID prices are jointly shifted such that the mean ID price lies 5% above the DA mean, that is, at 99.93 €/MWh, and 5% below, that is, at 90.42 €/MWh, respectively. These shifts are realistic given the historic distribution of ID/DA deviations.[81] Apart from the shift, the ID profiles have the same shape as in Figure 5.

*Link: https://git.rwth-aachen.de/avt-svt/public/representative-electricity-price-profiles (nominal daily profiles).

TABLE 5 Modified constraints in TEL-eNMPC. All other constraints are identical to Table 4.

	Variable	Unit	Type	Value set	Time set
(i)	N_{tank}	%	CV	$[0, 200]$	$\mathcal{T}_{\mathrm{c}}$
(ii)	N_{tank}	%	CV	$\{100\}$	$\{24\,\mathrm{h}\}$
(iii)	N_{tank}	%	CV	$\{N^{\mathrm{ids}}_{\mathrm{tank}}(t_0 + \tau_{\mathrm{c}})\}$	$\{t_0 + \tau_{\mathrm{c}}\}$

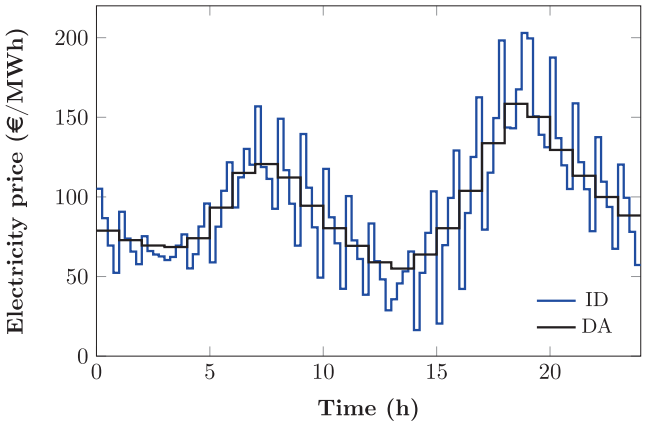

FIGURE 5 DA and ID price profiles. The average price of both profiles is 95.18 €/MWh.

5 | RESULTS AND DISCUSSION

In Section 5.1, we assess the economic revenue of an optimal steady-state operation subject to the different price profiles and different product purity grades. Section 5.2 discusses the results from the single-layer IDS and eNMPC strategies. Subsequently, we compare all results to the proposed TEL approach in Section 5.3. Lastly, we investigate the effect of a systematic ID price shift in Section 5.4. In the SI, we provide further material such as a collection of all results in a single table and additional plots.

5.1 | Optimal steady-state operation

We list the steady-state operating scenarios in Table 6. In this case study, scenario SS-DA-1500 is used as the reference case. Therein, the product quality is at its upper 1500 ppm impurity limit and the ASU production rate is 20 mol/s. The total energy demand over the full day is 7.12 kWh and the associated costs according to the DA prices are 677.94 €. Hereinafter, we compare all other strategies against this reference and provide the relative deviation of energy

TABLE 6 Results of steady-state operation.

Operating strategy	Price profile	I_{asu} (ppm)	Relative energy	
			Demand (%)	Costs (%)
Reference (SS-DA-1500)	DA	1500	±0.0	±0.0
SS-ID-1500	ID	1500	±0.0	±0.0
SS-DA-1000	DA	1000	+0.4	+0.4

TABLE 7 Results of (top-down) IDS with subordinate tNMPC. The percentages state the relative deviation from the SS-DA-1500 reference.

Operating strategy	Price profile	Relative energy	
		Demand (%)	Costs (%)
Reference	DA	±0.0	±0.0
IDS-DRTO	DA	+5.1	−1.2
IDS-tNMPC	DA	+5.5	−0.8

demand and costs in %. Since the DA and ID price profiles feature the same 24 h average price of 95.18 €/MWh, the results of SS-DA-1500 and SS-ID-1500 are identical.

In previous studies,[25,28] a steady state at 1000 ppm purity grade was considered as the nominal operating point due to constraint tracking limitations of linear MPC. This scenario corresponds to SS-DA-1000. As expected, an operation at higher product purity is associated with an increased energy consumption of 0.4%. Therefore, choosing an operation strategy able to operate the process close to its operating limits, for example, NMPC, is clearly economically advantageous even in the stationary case. Also, choosing a conservative benchmark such as SS-DA-1000 will render any proposed operating scheme seem more economical. Here, we challenge ourselves by selecting SS-DA-1500 as the nominal operating scenario.

5.2 | Single-layer strategies

We compare the top-down and bottom-up strategies, that is, IDS and eNMPC, respectively. We begin with an examination of the IDS results and place the findings in a process and problem context.

5.2.1 | IDS using tNMPC

Table 7 summarizes the energy consumption and economic performance. We distinguish two subcases. First, we consider the expected savings as given by solution of the IDS-DRTO problem (10). However, due to model errors of the SBM, the cost savings are lower when applying the schedule to the process (IDS-tNMPC, i.e., closed-loop results). Notice that the tank holdup at the end of the day reaches a slightly too low value in closed-loop operation due to scheduling errors. We account for this violation by adding the cost and energy needed to compensate for the missing product based on the SS-DA-1500 production costs.

Generally, the application of IDS realizes economic savings. Further, the respective values of IDS-DRTO and IDS-tNMPC are comparable. However, while the energy demand increases by approx. 5%, the economic revenue is relatively small, at a cost reduction only around 1%. Due to the less conservative steady-state benchmark and the moderate DA price profile, the savings achieved by the IDS strategy are less pronounced compared to Pattison et al. [25] and related works.

The closed-loop trajectories of the process under IDS and tNMPC are shown in Figure 6. In Figure 6A, we observe ASU production rates above the nominal production during periods of low electricity prices. Conversely, the production rate is reduced during high-price hours. Notably, while different intermediate production rates between 20 and 25 mol/s are observed, a decrease of the production rate is almost exclusively realized through a step to the 15 mol/s lower limit. The behavior is consistent with previous studies[25] and the periods of over- and underproduction are balanced. The presence of a noticeable share of nominal operation is explained by the high energy demand of liquefaction, introducing an economical threshold for overproduction and storage.

The product storage strategy is also visualized by Figure 6C. Interestingly, the tank is used for storage but never drained below the initial holdup of 100% reference storage, that is, 1.728 Mmol. The maximum storage during the scheduling period is +6.4% at 17 h. Hence, a considerably smaller storage tank may be designed in practice.

Figure 6B depicts the total power consumption of ASU and storage system. The steps associated with an increased production, that is, 2 to 4 h and 11 to 16 h, include the activation or deactivation of the liquefaction system. Therefore, deviations from the nominal power demand are asymmetric. Moreover, Figure 6D confirms that IDS is able to satisfy the product quality constraint. Due to the overestimation of the product impurity by the SBM, see also Figure 4A, the upper bound is never reached.

5.2.2 | ENMPC

Next, we assess single-layer eNMPC in combination with either DA or ID prices. To this end, we investigate different prediction horizon τ_c as listed in Table 8. We adjust the control step lengths Δt_u to obtain a degree of freedom (DOF) of the same magnitude in all control problems. Thereby, we limit the computational effort of eNMPC. The maximum value of $\Delta t_u = 15$ min agrees with the MV parameterization in previous works.[28,82] In Schäfter et al. ,[41] the authors even used $\Delta t_u = 60$ min.

We begin with eNMPC using DA prices. As seen in Table 8, single-layer eNMPC with a short prediction horizon below 6 h only

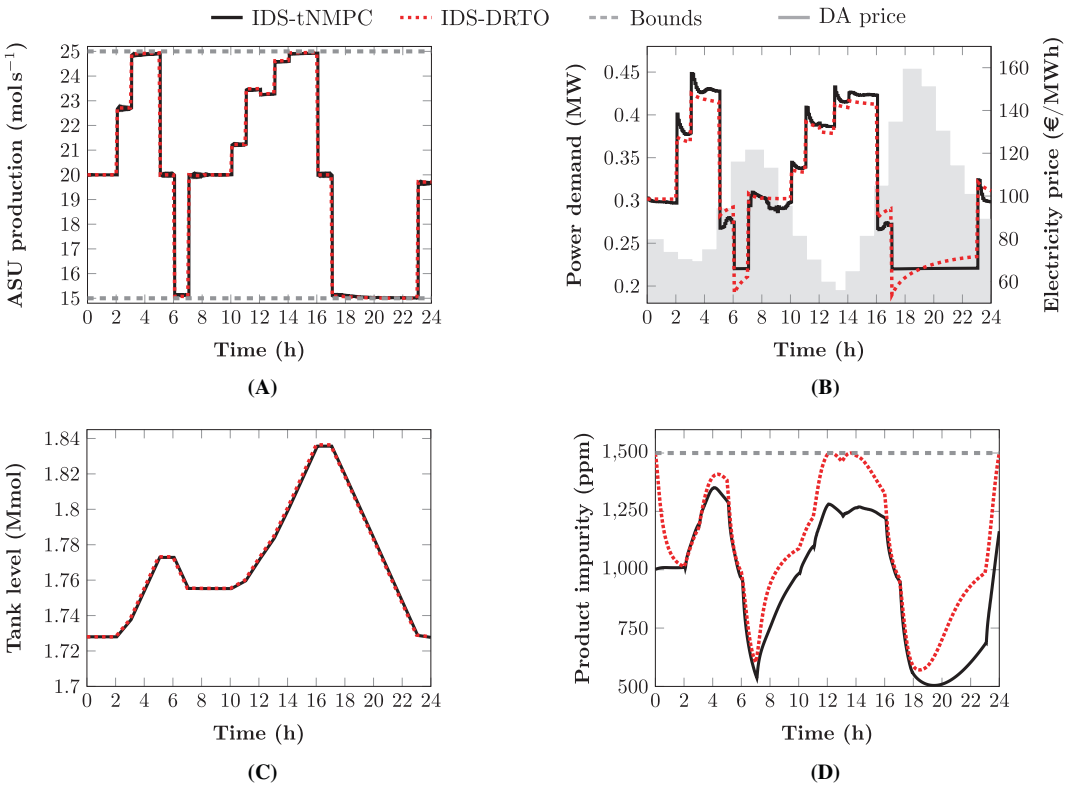

FIGURE 6 Closed-loop process response under IDS and tNMPC. (a) ASU production rate, (b) total power consumption, (c) storage tank holdup, (d) product quality.

TABLE 8 Results of (bottom-up) eNMPC using DA or ID prices. The percentages state the relative deviation from the SS-DA-1500 reference.

Operating strategy	$\mathcal{T}_c$ (h)	Δt_u (min)	DOF per MV	Relative energy	
				Demand (%)	Costs (%)
Reference	–	–	–	±0.0	±0.0
DA-2	2	5	24	+0.1	−0.1
DA-3	3	5	36	+0.8	−0.3
DA-4	4	7.5	32	+0.9	−0.5
DA-6	6	7.5	48	+1.9	−1.5
DA-9	9	15	36	+3.0	−2.0
DA-12	12	15	48	+2.7	−2.4
ID-2	2	5	24	+1.9	−2.4
ID-3	3	5	36	+2.5	−3.1
ID-4	4	7.5	32	+2.5	−3.5
ID-6	6	7.5	48	+3.8	−4.3
ID-9	9	15	36	+4.6	−4.3
ID-12	12	15	48	+4.0	−4.4

generates a profit below 1%. For longer prediction horizons, eNMPC outperforms IDS, while having a lower power demand. The results suggest that profit primarily depends on the prediction horizons and increases with τ_c. In addition, we suspect a correlation of DOF and energy demand, where energy demand reduces with higher DOF.

Figure 7 visualizes key closed-loop trajectories of the process operated by eNMPC using DA prices. As visible in Figure 7A, short-horizon eNMPC (DA-2) does not excite the system notably around the nominal operating point, which is also reflected in the total power consumption, see Figure 7B, and storage tank holdup in Figure 7C. The short-term excitation as present for DA-2 is likely to stress process equipment but does not realize an economic profit. Clearly, the combination of short prediction horizon and slow DA price trends is ineffectual.

On the other hand, long-horizon eNMPC (DA-12) accomplishes a significant economic benefit by operating the process flexibly and making use of a large part of the admissible operating range, Figure 7A. Similar to IDS, the process is operated around the nominal production rate of 20 mol/s and there exist distinct periods of non-nominal operation, visible in Figure 7A,B. However, we observe a larger share of intermediate production rates between the lower and upper limit that are incrementally changed between short periods. This behavior was also observed by Caspari et al. [28] and is explained by the shorter control intervals and online feedback to the economic controller.

While DA-2 operates the process near the upper impurity limit, DA-12 intermediately drives the process to higher product purity. There, over-purification is seen during periods of underproduction, while reaching 1500 ppm when increasing production as well as at

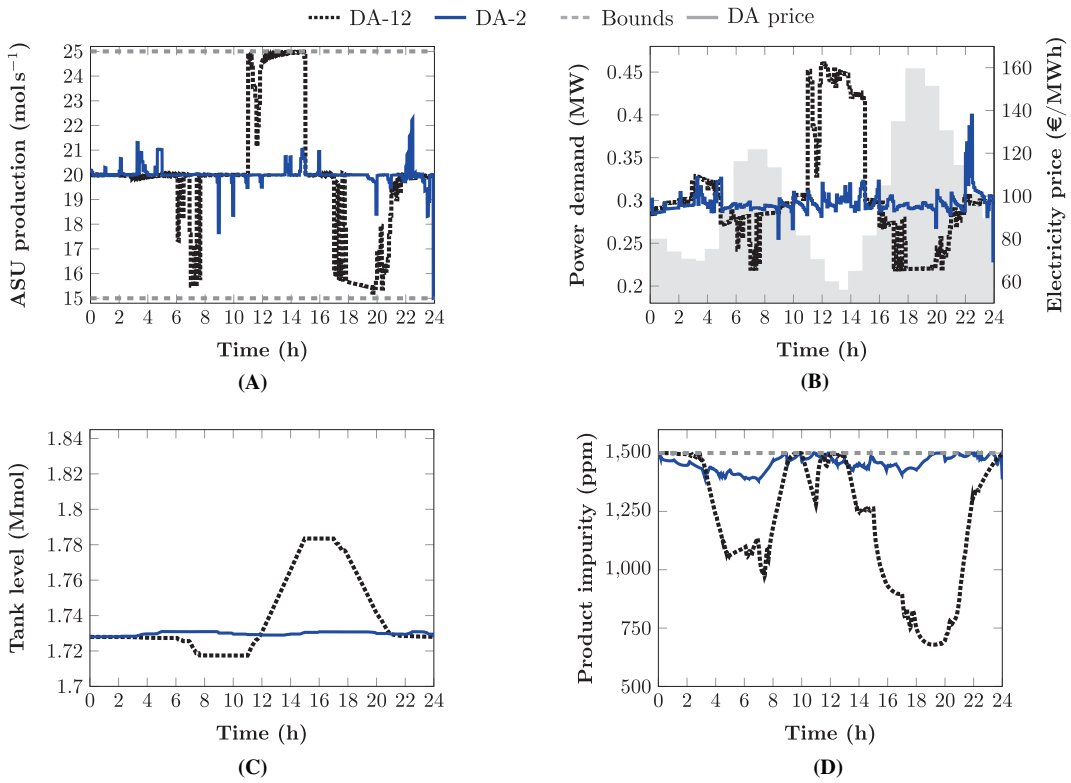

FIGURE 7 Closed-loop process response under eNMPC and DA prices. (a) ASU production rate, (b) total power demand, (c) storage tank holdup, (d) product quality.

the end of the day. Further, compared to the one-sided usage of the tank by IDS, the DA-12 eNMPC strategy drains and fills the tank in both directions around the nominal holdup, Figure 7C.

Next, we assess single-layer eNMPC in combination with ID prices. As for the eNMPC-DA combination, longer prediction horizons are economically beneficial, Table 8. However, the economic profit is generally higher for the ID profile, outperforming eNMPC-DA in all configurations. The maximum relative savings of 4.4% are provided by the ID-12 configuration. Comparing the DA and ID price profiles in Figure 5 underpins the wider range, stronger fluctuation, and higher frequencies in the ID profile over one day. Similar to Caspari et al. ,[28] we conclude that a wide-range high-fluctuation price profile is economically advantageous in the context of a single-layer eNMPC strategy.

Figure 8 presents the closed-loop process response in the ID scenarios. Compared to the IDS and eNMPC-DA setups, the process is operated more dynamically and aggressively, Figure 8A,B. In particular, a short-term increase and decrease of the production rate around the nominal point is visible in every hour. Compared to ID-2, the periods of increased or decreased production are longer for ID-12. Given the storage tank hold-up constraint in Table 4, the near-nominal operation by ID-2 is not surprising and also reflected in the nearly constant tank holdup, Figure 8C. Further, the amounts of product stored and withdrawn from the tank are comparable to the eNMPC-DA configurations in Figure 7C. Likewise, the product impurity trajectories in Figure 8D follow a similar trend as in Figure 7D. However, the more aggressive process manipulation by eNMPC-ID is visible in the form of several "spikes" in the profiles. Finally, the slight violations of the purity bounds are attributed to feasibility tolerances.

5.3 | Two economic layers

We finally examine the proposed TEL scheme. Similar to single-layer eNMPC, we consider different prediction horizons and control intervals for the lower-layer eNMPC in the TEL strategy. Since the configurations are the same as in Table 8, we only state the control horizon in Table 9. We provide the CPU costs of lower-layer eNMPC in the Appendix. The upper-layer IDS is identical to the single-layer application and thus the schedule in Table 7 remains valid.

From Table 9 we observe that the overall cost savings and energy demand appear to be uncorrelated with the eNMPC horizon. Hence, there is no practical benefit from using a prediction horizon above 2 h. We attribute the variance in the individual results to differences in the control grid and numerical convergence.

Figure 9 depicts the closed-loop trajectories of the process operated by the TEL scheme. Since all configurations are comparably economical, we only show the results of TEL-2. In addition, the trajectories as scheduled by the upper-layer IDS are identical to Figure 6. The closed-loop ASU production rate in Figure 9A exhibits a significant deviation from the schedule in Figure 6 and is more comparable to the eNMPC results in Figure 8. The same applies for the total

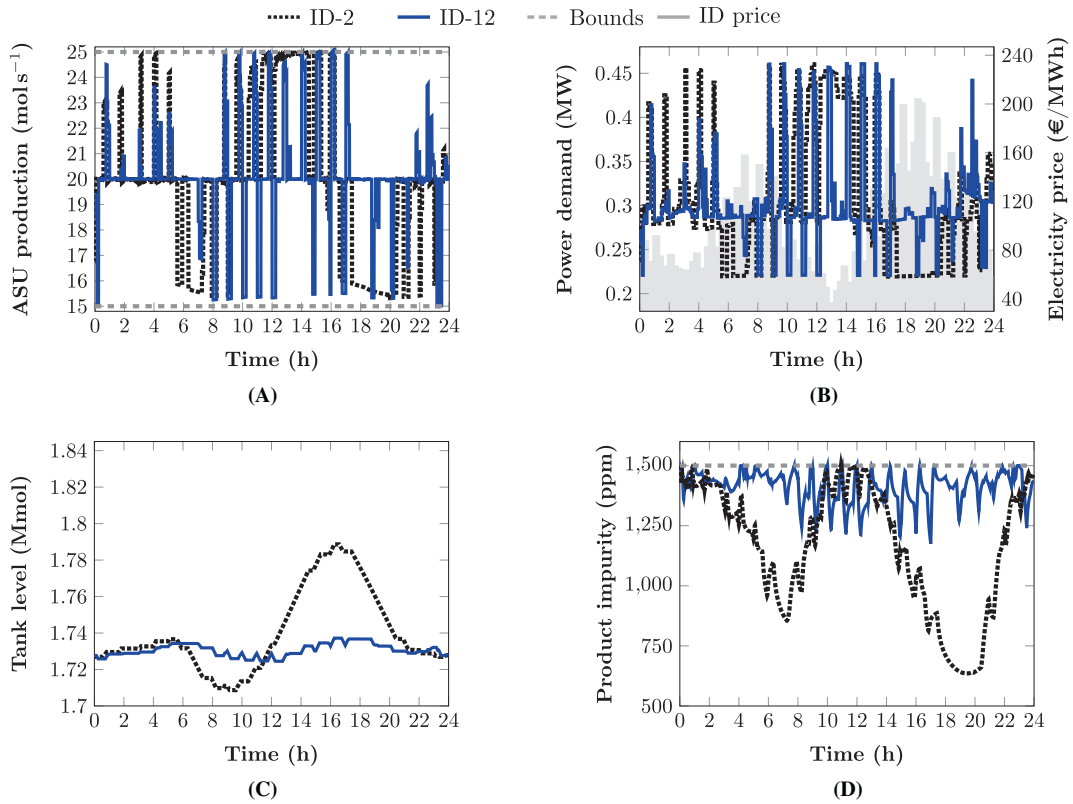

FIGURE 8 Closed-loop process response under eNMPC and ID prices. (a) ASU production rate, (b) total power demand, (c) storage tank holdup, (d) product quality.

TABLE 9 Results the two-layer scheme combining IDS and eNMPCs. The percentages state the relative deviation from the SS-DA-1500 reference.

Operating strategy	$\mathcal{T}_c$ (h)	Relative energy	
		Demand (%)	Costs (%)
Reference	–	±0.0	±0.0
TEL-2	2	+4.7	−4.1
TEL-3	3	+4.4	−4.1
TEL-4	4	+4.4	−4.3
TEL-6	6	+4.5	−4.4
TEL-9	9	+4.7	−3.8
TEL-12	12	+4.6	−4.0

power consumption, shown in Figure 9B. However, we notice extended periods of operation near the upper and lower production rate limit during the 12 to 14 h and 17 to 21 h, respectively. During these periods, the scheduled storage tank holdup changes considerably, Figure 9C. Due to the terminal holdup constraints in the lower-layer eNMPC problem, the closed-loop trajectories must follow the scheduled tank holdup closely, necessitating in the periods of minimum and maximum production. Notice that in preliminary studies, eNMPC encountered feasibility problems when removing the terminal holdup constraint. Figure 9D shows the product quality response, which exhibits similar characteristics as for eNMPC-ID in Figure 8D.

In Figure 10, we illustrate the trading behavior of the TEL scheme. Therein, $\Delta E(t)$ denotes the cumulative traded energy (MWh) over the respective 15 min interval, $i = 1, 2, \ldots, 96$, rather than the instantaneous power in MW. The traded energy $\Delta E(t)$ is calculated as:

$$\Delta E(t) = -\int_{t_i}^{t_i+15\ \text{min}} \Delta P(\tau)\, \mathrm{d}\tau,\ t \in [t_i, t_i + 15\ \text{min}), \tag{13}$$

where $\Delta P(t)$ corresponds to Equation (12). Positive values of ΔE correspond to energy offer and negative values to purchase. Moreover, the price difference $\mathcal{C}^{\Delta}(t)$ is defined by $\mathcal{C}^{\Delta}(t) = \mathcal{C}^{\mathrm{ID}}(t) - \mathcal{C}^{\mathrm{DA}}(t)$. As expected, energy is purchased if $\mathcal{C}^{\Delta}(t) < 0$ and offered otherwise. For $\mathcal{C}^{\Delta}(t) \approx 0$, the traded energy volumes are close to zero. During the 17 to 21 h, the trading behavior does not follow the described mechanism and the trading curve is fairly smooth. Again, we explain this exception by the eNMPC terminal storage tank constraint in combination with the strong holdup decrease scheduled by IDS, cf. Figure 9C. During this period, the terminal constraint tracking exhausts all degrees of freedom and thereby constrains the trading. For TEL-2, the additional profit from arbitrage amounts to 3.3% of the nominal operating costs.

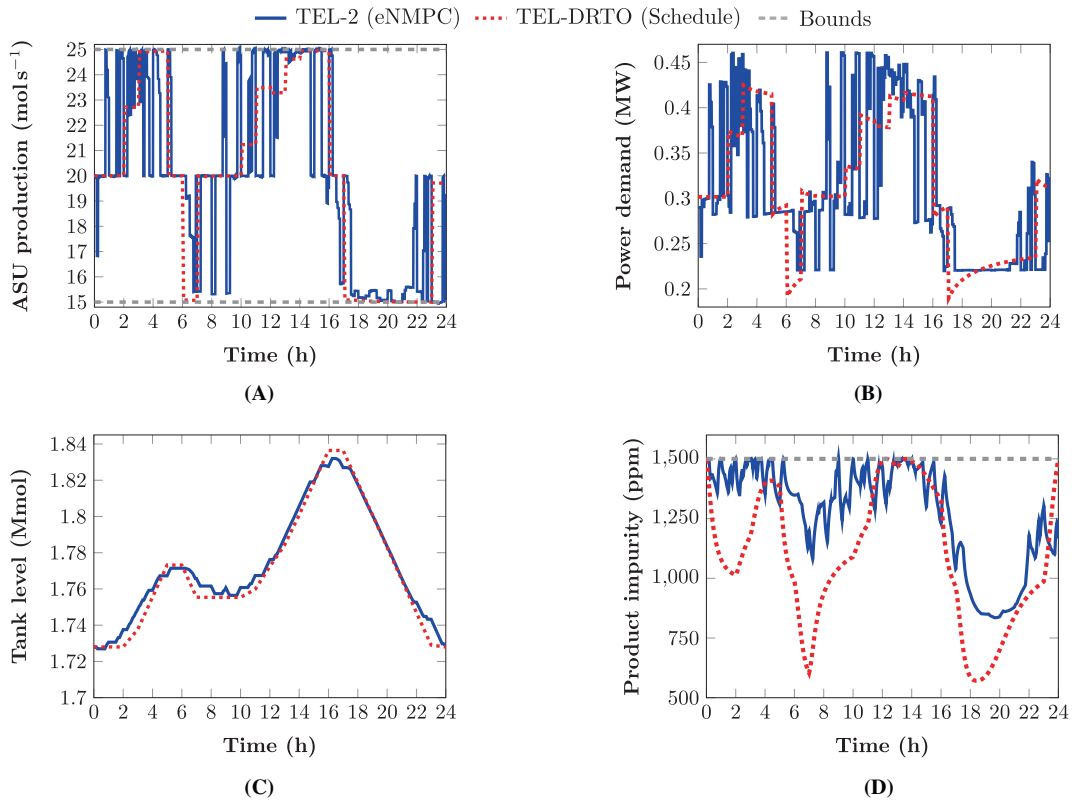

FIGURE 9 Closed-loop process response under two-layer IDS and eNMPC. (a) ASU production rate, (b) total power consumption, (c) storage tank holdup, (d) product quality.

FIGURE 10 Energy volumes purchased ($\Delta E(t) < 0$) or offered ($\Delta E(t) > 0$) by the two-layer strategy.

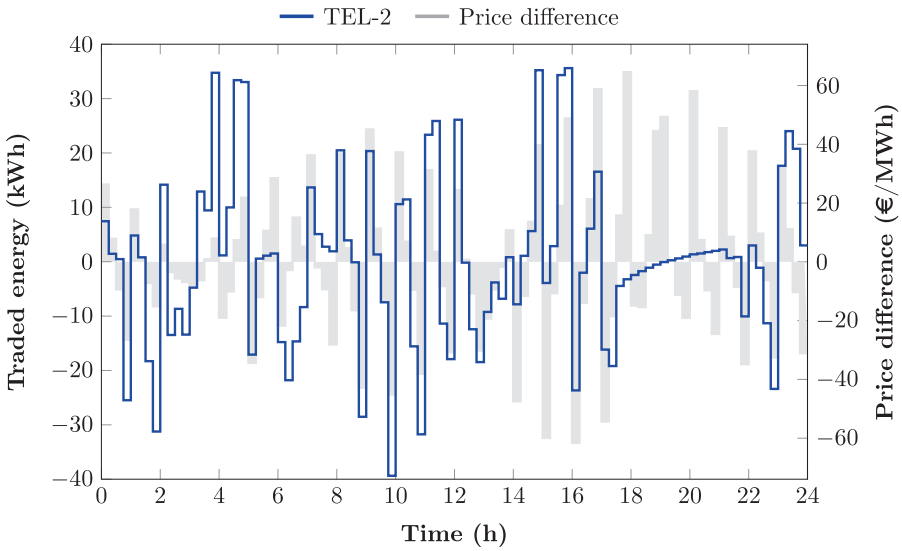

5.4 | Shifted ID price scenario

In this second study, we consider two alternative price scenarios that are modifications of the DA and ID profiles from the first study. The first scenario, denoted by $ID_{\oplus}$, is obtained by a constant positive shift of all ID prices such that the mean ID price is 5% higher than the mean DA price. Similarly, we consider a price scenario $ID_{\ominus}$, where the mean ID price is 5% below the mean DA price. We apply all operating strategies to these two scenarios and collect the economic results in Table 10. Since the DA profile does not change, the IDS and eNMPC-DA results in Tables 7 and 8 remain valid.

First, we emphasize that we continue to compare against the SS-DA-1500 reference. However, we additionally examine the counterpart to SS-ID-1500 using $ID_{\oplus}$ or $ID_{\ominus}$ prices. Due to the generally higher price level of $ID_{\oplus}$, we must expect a lower profit of eNMPC-ID and TEL. Indeed, the costs for eNMPC-ID are shifted to positive

TABLE 10 Results in the second and third price scenarios. The percentages state the relative deviation from the SS-DA-1500 reference.

Operating strategy	τ_c (h)	Scenario ⊕		Scenario ⊖	
		Relative energy		Relative energy	
		Demand (%)	Costs (%)	Demand (%)	Costs (%)
Reference	–	±0.0	±0.0	±0.0	±0.0
SS-ID-1500	–	±0.0	+5.0	±0.0	−5.0
ID-2	2	+1.8	+2.7	+2.2	−7.5
ID-3	3	+2.2	+2.0	+2.7	−8.4
ID-4	4	+2.2	+1.8	+2.7	−8.7
ID-6	6	+3.5	+0.9	+4.1	−9.6
ID-9	9	+4.6	+1.5	+4.8	−9.5
ID-12	12	+3.7	+0.7	+4.1	−9.7
TEL-2	2	+4.8	−4.0	+4.9	−2.5
TEL-3	3	+4.4	−4.1	+5.0	−2.4
TEL-4	4	+4.3	−4.1	+4.6	−4.0
TEL-6	6	+4.3	−4.4	+5.0	−4.4
TEL-9	9	+4.5	−3.8	+4.9	−3.9
TEL-12	12	+4.4	−4.0	+4.7	−4.0

values, indicating higher expenses compared to the steady-state operation with energy products from the DA market. We observe $\geq 0.7\%$ cost increase over the stationary DA reference. As before, the long-horizon eNMPC configurations realize better economic results than short-horizon eNMPC. When compared to SS-ID$_\oplus$-1500, the eNMPC-ID strategy, however, generates economic savings. In fact, eNMPC-ID follows nearly the same operating strategy as before, only on a higher price level. We provide the respective closed-loop trajectories in the SI.

As opposed to stand-alone eNMPC-ID, the TEL strategy realizes economic profit comparable to the first case study, despite the higher price level of ID$_\oplus$. Moreover, the cost savings remain independent of the TEL-eNMPC prediction horizon, wherefore we may use a short horizon. Compared to SS-ID$_\oplus$-1500 the TEL cost savings are even as high as 9.4%.

In the case of a systematic ID price shift in negative direction, the savings are reversed. Due to the absence of a scheduling layer, stand-alone eNMPC has no commitments regarding DA products and can fully benefit from lower ID$_\ominus$ prices. As a consequence, eNMPC generates up to 9.7% revenue compared to the SS-DA-1500 reference. On the other hand, the energy volumes purchased on the DA market constrain the economic profit of the TEL strategy. Yet, remarkably, the TEL scheme continues to realize a benefit of up to 4.4% compared to the SS-DA-1500 reference. We notice that a slightly longer TEL-eNMPC horizon of 4 h is required here to realize savings of 4%.

5.5 | Overall comparison

We summarize the findings from the case study. Figure 11 extracts the key trends from Tables 6 to 9 and compares the different operating strategies in the first price scenario. In all cases, we see a positive increase in energy demand, that is, flexible process operation consumes more power than steady-state operation. At the same time, the operating strategies achieve different profit, with single-layer IDS providing little savings at the highest energy demand. The economic profit from single-layer eNMPC strongly depends on the prediction horizon and the availability of a reliable price forecast over this horizon. Moreover, eNMPC-ID outperforms eNMPC-DA due to a stronger variance in the ID profile compared to DA prices. We account the dependence of profit on the prediction horizon to the price variance rather than to the process dynamics. Figure 4 indicates that the closed-loop settling time is ≈ 2 h. In contrast, the principal frequency of the price profiles in Figure 5 is $f_0 \approx 1/12\,\mathrm{h}^{-1}$. Consequently, a larger horizon covers a larger price range to be leveraged in optimization.

The TEL scheme achieves similar savings as the long-horizon eNMPC-ID configurations. At the same time, a significantly shorter TEL-eNMPC prediction horizon τ_c than in single-layer eNMPC enables similar savings. This finding is consistent with the above discussion as the upper-layer TEL-IDS already covers the slower price trends at f_0 and the TEL-eNMPC optimizes around this reference using the considerably faster ID-DA deviations of principal frequency $f_1 \approx 1/2\,\mathrm{h}^{-1}$, see Figure 5. Hence, a shorter horizon is sufficient. Notably, the major share of economic profit is due to arbitrage, as clear from comparing IDS and TEL in Figure 11. For further information on the principal frequencies see References 45, 86.

A short eNMPC horizon is practically beneficial for two reasons. First, a long horizon is generally associated with high online CPU costs and computational delay. The comparison of the CPU costs of stand-alone eNMPC and TEL-eNMPC in the SI confirms this trend. As we aim for fast control updates, we thus prefer short horizons. Second, price prediction uncertainty generally grows with longer horizons,[87,88]

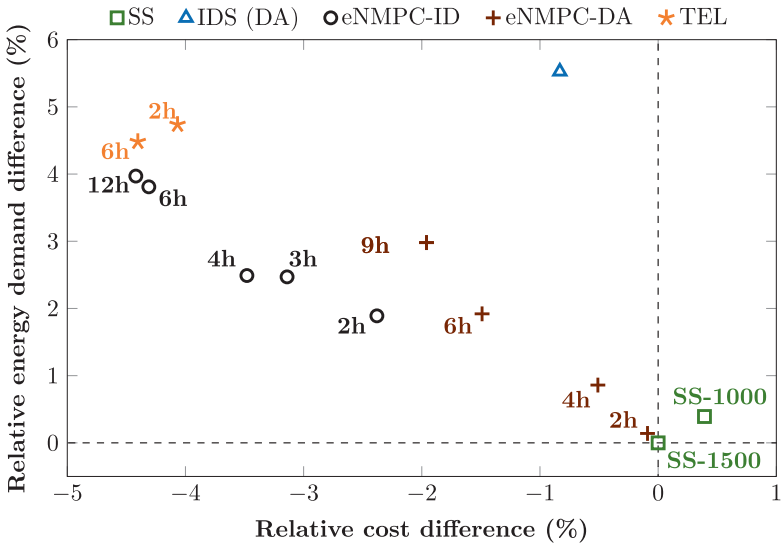

FIGURE 11 Relative cost savings and energy demand of single-economic-layer and TEL operating strategies compared to steady-state operation. The time values indicate the eNMPC prediction horizon.

irrespective that herein we have assumed the exact knowledge of future ID prices. In particular, for short eNMPC horizons we can expect fairly reliable short-term ID forecast, whereas an eNMPC strategy based on 12 h predictions may suffer from price uncertainty. We thus regard the short eNMPC horizons in the TEL strategy as advantage in regards of economic robustness. We will investigate this effect more in-depth in future works.

In the second and third price scenarios, the TEL schemes proves to be economically robust against systematic price shifts between the DA and ID markets. At the same time, the economic performance of stand-alone eNMPC-ID is more sensitive to the price differences due to the sole dependency on the ID profile. As a result, stand-alone eNMPC and TEL outperform each other in one scenario each. Clearly, the commitment to DA energy products provides an economic fallback in the case of high ID prices, but also constrains the TEL revenue in case of considerably lower ID prices. However, the TEL approach succeeds to realize a nearly constant economic revenue in all scenarios, whereas stand-alone eNMPC even results in a cost increase relative to the steady-state DA reference. Overall, TEL is the only scheme that realizes savings in all price scenarios.

6 | CONCLUSIONS AND OUTLOOK

We propose an integrated scheduling and control approach with two economic layers, termed TEL, for energy flexible operation of chemical production processes. Therein, we combine dynamic scheduling and eNMPC to profit from fluctuating energy prices and price differences between DA auction and continuous ID markets. The approach unites several advantages of the individual approaches. First, IDS is executed offline and thus allows for long scheduling horizons, that is, planning one or multiple days ahead, which is not computationally feasible for stand-alone eNMPC. By considering "long-term" production goals, IDS increases flexibility and provides an economically optimized operating trajectory. Second, employing lower-layer eNMPC enables economic disturbance rejection as well as rapid response to unexpected market fluctuations, thereby providing an advantage over stand-alone IDS.

In a case study, we compared the proposed TEL scheme with state-of-the-art single-layer approaches and demonstrated high savings and economic robustness of our method. For all methods, the price differences in a moderate scenario constructed from historical European price data were sufficient to incentivize DSM and intermittently overproduce and store liquid gas product. In general, flexibilization is associated with an increased energy consumption compared to steady-state operation. At the same time, the strategies investigated realize different revenues, with IDS and short-horizon eNMPC showing the worst performance. The economic profit from single-layer eNMPC strongly depends on a long prediction horizon, a reliable price forecast, and the DA/ID price levels. Conversely, the proposed TEL strategy consistently provides high savings in all price scenarios and is therefore economically promising. By participating in two markets, the TEL strategy enables the plant operator to benefit from arbitrage, that is, buying on one market and selling on another. Importantly, the prediction horizon of eNMPC in the TEL setup can be chosen considerably shorter than in a stand-alone eNMPC application, whereby computational tractability and price prediction accuracy may be considerably improved.

In the present study, we did not investigate the effect of process disturbances on the performance of the competing schemes. In fact, unpredictable disturbances are rather uncommon for ASUs. Generally, stand-alone eNMPC performs disturbance rejection within the regular economic optimization. Conversely, a correction of the schedule in IDS necessitates trading on the ID market to update the DA schedule. The disturbance rejection features of eNMPC are inherited by the TEL scheme. Performing economic disturbance rejection in the lower layer of a two-layer economic scheme has already been discussed in the literature.[47–49] However, in the case of infrequent but large disturbances, a recomputation of the top-layer schedule over the longer scheduling horizon may offer additional benefits.

Future work should extend the approach to multi-product processes and variable product grades. Using a "power-tracking NMPC" instead of production rate tracking as well as reference trajectory tracking instead of setpoint tracking may further improve the economic performance of the scheme. Additionally, accounting for the ID market in the day-ahead IDS problem as well as applying stochastic ID price forecasting in either integration approach may enable further benefits. Finally, modeling and optimization strategies for IDS with hard-constrained lower-layer controllers are needed.

AUTHOR CONTRIBUTIONS

Jan C. Schulze: conceptualization; methodology; software; validation; formal analysis; writing – original draft; visualization. **Chrysanthi Papadimitriou:** investigation; software; validation; formal analysis; writing – original draft; visualization. **Paul Kolmer:** investigation; software. **Alexander Mitsos:** funding acquisition; project administration; resources; writing – review and editing; validation; supervision.

ACKNOWLEDGEMENTS

The authors gratefully acknowledge the financial support of the Kopernikus project SynErgie by the Federal Ministry of Education and Research (BMBF), and the project supervision by the project management organization Projektträger Jülich (PtJ). They additionally acknowledge the financial support of and the Deutsche Forschungsgemeinschaft (DFG, German Research Foundation)-333849990/GRK2379 (IRTG Hierarchical and Hybrid Approaches in Modern Inverse Problems). The authors thank Pascal Schäfer, Sonja Germscheid, and Mohammad El Wajeh for their thoughts on the article and careful reading. Open Access funding enabled and organized by Projekt DEAL.

AUTHOR CONTRIBUTIONS

Jan C. Schulze: conceptualization, methodology, software, validation, formal analysis, writing-original draft, visualization. **Chrysanthi Papadimitriou:** investigation, software, validation, formal analysis, writing-original draft, visualization. **Paul Kolmer:** software, investigation. **Alexander Mitsos:** supervision, validation, writing – review & editing, resources, project administration, funding acquisition.

CONFLICTS OF INTEREST STATEMENT

There are no conflicts of interest.

DATA AVAILABILITY STATEMENT

The data that supports the findings of this study are available in the supplementary material of this article. The data is provided in `csv` format and comprises the full data of all plotted figures. The code for reproducing the published results is available from the corresponding author upon reasonable request. All simulations were executed multiple times to ensure reliability and reproducibility of the data.

ORCID

Jan C. Schulze https://orcid.org/0000-0001-5048-1779
Alexander Mitsos https://orcid.org/0000-0003-0335-6566

REFERENCES

1. Becerra VM, Roberts PD, Griffiths GW. Novel developments in process optimisation using predictive control. *J Process Control*. 1998; 8(2):117-138.
2. Backx T, Bosgra O, Marquardt W. Integration of model predictive control and optimization of processes: Enabling technology for market driven process operation. *IFAC Proc Vol*. 2000;33(10):249-260.
3. Flores-Tlacuahuac A, Grossmann IE. Simultaneous cyclic scheduling and control of a multiproduct CSTR. *Ind Eng Chem Res*. 2006;45(20): 6698-6712.
4. Mitsos A, Asprion N, Floudas CA, et al. Challenges in process optimization for new feedstocks and energy sources. *Comput Chem Eng*. 2018;113:209-221.
5. Bruns B, Di Pretoro A, Grünewald M, Riese J. Indirect demand response potential of large-scale chemical processes. *Ind Eng Chem Res*. 2022;61(1):605-620.
6. Tosukhowong T, Lee JM, Lee JH, Joseph L. An introduction to a dynamic plant wide optimization strategy for an integrated plant. *Comput Chem Eng*. 2004;29(1):199-208.
7. Engell S. Feedback control for optimal process operation. *J Process Control*. 2007;17(3):203-219.
8. Fritsch P, Hoffmann R, Flüggen R, et al. Distributed temperature and strain measurements at a cryogenic plate-fin heat exchanger test rig. *Chem Ing Tech*. 2022;94(4):555-562.
9. Caspari A, Offermanns C, Schäfer P, Mhamdi A, Mitsos A. A flexible air separation process: 1. Design and steady-state optimizations. *AICHE J*. 2019;65(11):e16705.
10. Castro PM, Ave GD, Engell S, Grossmann IE, Harjunkoski I. Industrial demand side management of a steel plant considering alternative power modes and electrode replacement. *Ind Eng Chem Res*. 2020; 59(30):13642-13656.
11. Cao Y, Swartz CLE, Flores-Cerrillo J. Optimal dynamic operation of a highpurity air separation plant under varying market conditions. *Ind Eng Chem Res*. 2016;55(37):9956-9970.
12. El Wajeh M, Mhamdi A, Mitsos A. Optimal design and flexible operation of a fully electrified biodiesel production process. *Ind Eng Chem Res*. 2024;63(3):1487-1500.
13. Baldea M, Harjunkoski I. Integrated production scheduling and process control: A systematic review. *Comput Chem Eng*. 2014;71:377-390.
14. Ellis M, Durand H, Christofides PD. A tutorial review of economic model predictive control methods. *J Process Control*. 2014;24(8): 1156-1178.
15. Helbig A, Abel O, Marquardt W. Structural concepts for optimization based control of transient processes. *Nonlinear Model Predictive Control*. Birkhäuser Basel; 2000:295-311.
16. Chatzidoukas C, Kiparissides C, Perkins JD, Pistikopoulos EN. Optimal grade transition cam710 paign scheduling in a gas-phase polyolefin FBR using mixed integer dynamic optimization. *Process Systems Engineering 2003, 8th International Symposium on Process Systems Engineering*. Computer Aided Chemical Engineering. Vol 15. Elsevier; 2003:744-747.
17. Mahadevan R, Doyle FJ, Allcock AC. Control-relevant scheduling of polymer grade transitions. *AICHE J*. 2002;48(8):1754-1764.
18. Chu Y, You F. Integration of scheduling and control with online closed-loop implementation: Fast computational strategy and large-scale global optimization algorithm. *Comput Chem Eng*. 2012;47: 248-268.
19. Jamaludin MZ, Swartz CLE. Closed-loop Formulation for Nonlinear Dynamic Real-time Optimization. *IFAC-PapersOnLine*. 2016;49(7): 406-411.
20. Simkoff JM, Baldea M. Production scheduling and linear MPC: Complete integration via complementarity conditions. *Comput Chem Eng*. 2019;125:287-305.
21. Schulze JC, Caspari A, Offermanns C, Mhamdi A, Mitsos A. Nonlinear model predictive control of ultra-high-purity air separation units using

transient wave propagation model. *Comput Chem Eng*. 2021;145:107163.

22. Schulze JC, Doncevic DT, Erwes N, Mitsos A. Data-Driven Model Reduction and Nonlinear Model Predictive Control of an Air Separation Unit by Applied Koopman Theory. *Foundations of Computer Aided Process Operations / Chemical Process Control (FOCAPO)*. Computer Aids for Chemical Engineering; 2023.
23. Mitrai I, Daoutidis P. A multicut generalized benders decomposition approach for the integration of process operations and dynamic optimization for continuous systems. *Comput Chem Eng*. 2022;164:107859.
24. Nie Y, Biegler LT, Villa CM, Wassick JM. Discrete Time Formulation for the Integration of Scheduling and Dynamic Optimization. *Ind Eng Chem Res*. 2015;54(16):4303-4315.
25. Pattison RC, Touretzky CR, Johansson T, Harjunkoski I, Baldea M. Optimal process operations in fast-changing electricity markets: framework for scheduling with low-order dynamic models and an air separation application. *Ind Eng Chem Res*. 2016;55(16):4562-4584.
26. Kumar P, Rawlings JB, Wright SJ. Industrial, large-scale model predictive control with structured neural networks. *Comput Chem Eng*. 2021;150:107291.
27. Mitrai I, Daoutidis P. Computationally efficient solution of mixed integer model predictive control problems via machine learning aided Benders Decomposition. *J Process Control*. 2024;137:103207.
28. Caspari A, Tsay C, Mhamdi A, Baldea M, Mitsos A. The integration of scheduling and control: Top-down vs. Bottom-up. *J Process Control*. 2020;91:50-62.
29. Angeli D, Amrit R, Rawlings JB. On average performance and stability of economic model predictive control. *IEEE Trans Autom Control*. 2011;57(7):1615-1626.
30. Daoutidis P, Lee JH, Harjunkoski I, Skogestad S, Baldea M, Georgakis C. Integrating operations and control: A perspective and roadmap for future research. *Comput Chem Eng*. 2018;115:179-184.
31. Ierapetritou MG, Wu D, Vin J, Sweeney P, Chigirinskiy M. Cost minimization in an energy intensive plant using mathematical programming approaches. *Ind Eng Chem Res*. 2002;41(21):5262-5277.
32. Karwan MH, Keblis MF. Operations planning with real time pricing of a primary input. *Comput Oper Res*. 2007;34(3):848-867.
33. Miller J, Luyben WL, Blouin S. Economic incentive for intermittent operation of air separation plants with variable power costs. *Ind Eng Chem Res*. 2008;47(4):1132-1139.
34. Otashu JI, Baldea M. Demand response-oriented dynamic modeling and operational optimization of membrane-based chlor-alkali plants. *Comput Chem Eng*. 2019;121:396-408.
35. Brée LC, Perrey K, Bulan A, Mitsos A. Demand side management and operational mode switching in chlorine production. *AICHE J*. 2019;65(7):e16352.
36. Cegla M, Semrau R, Tamagnini F, Engell S. Flexible process operation for electrified chemical plants. *Curr Opin Chem Eng*. 2023;39:100898.
37. Kazemi M, Zareipour H, Amjady N, Rosehart WD, Ehsan M. Operation scheduling of battery storage systems in joint energy and ancillary services markets. *IEEE Trans Sustain Energy*. 2017;8(4):1726-1735.
38. Schäfer P, Westerholt HG, Schweidtmann AM, Ilieva S, Mitsos A. Model-based bidding strategies on the primary balancing market for energy-intense processes. *Comput Chem Eng*. 2019;120:4-14.
39. Otashu JI, Baldea M. Grid-level "battery" operation of chemical processes and demandside participation in short-term electricity markets. *Appl Energy*. 2018;220(3):562-575.
40. Meese J, Dahlmann B, Zdrallek M, Voelschow A. Intraday Redispatch - Optimal scheduling of industrial processes at day-ahead and continuous intraday market. *International ETG Congress 2017*. VDE; 2017:1-6.
41. Schäfer P, Caspari A, Mhamdi A, Mitsos A. Economic nonlinear model predictive control using hybrid mechanistic data-driven models for optimal operation in real-time electricity markets: In-silico application to air separation processes. *J Process Control*. 2019;84:171-181.
42. Simkoff JM, Baldea M. Stochastic scheduling and control using data-driven nonlinear dynamic models: Application to demand response operation of a Chlor-Alkali plant. *Ind Eng Chem Res*. 2020;59(21):10031-10042.
43. Dowling AW, Kumar R, Zavala VM. A multi-scale optimization framework for electricity market participation. *Appl Energy*. 2017;190(1):147-164.
44. Hedegaard RE, Pedersen TH, Petersen S. Multi-market demand response using economic model predictive control of space heating in residential buildings. *Energ Build*. 2017;150:253-261.
45. Germscheid SHM, Mitsos A, Dahmen M. Demand response potential of industrial processes considering uncertain short-term electricity prices. *AICHE J*. 2022;68(11):e17828.
46. Varelmann T, Erwes N, Schäfer P, Mitsos A. Simultaneously optimizing bidding strategy in pay-as-bid-markets and production scheduling. *Comput Chem Eng*. 2022;157:107610.
47. Würth L, Hannemann R, Marquardt W. A two-layer architecture for economically optimal process control and operation. *J Process Control*. 2011;21(3):311-321.
48. Alanqar A, Durand H, Albalawi F, Christofides PD. An economic model predictive control approach to integrated production management and process operation. *AICHE J*. 2017;63(6):1892-1906.
49. Clarke WC, Manzie C, Brear MJ. Hierarchical economic MPC for systems with storage states. *Automatica*. 2018;94:138-150.
50. Rawlings JB, Mayne DQ, Diehl M. *Model Predictive Control: Theory, Computation, and Design*. 2nd ed. Nob Hill Publishing; 2017.
51. Grüne L, Pannek J. *Nonlinear Model Predictive Control*. Springer; 2017.
52. Zhu Y, Legg S, Laird CD. A multiperiod nonlinear programming approach for operation of air separation plants with variable power pricing. *AICHE J*. 2011;57(9):2421-2430.
53. Mitra S, Grossmann IE, Pinto JM, Arora N. Optimal production planning under time-sensitive electricity prices for continuous power-intensive processes. *Comput Chem Eng*. 2012;38:171-184.
54. Zhang Q, Grossmann IE, Heuberger CF, Sundaramoorthy A, Pinto JM. Air separation with cryogenic energy storage: optimal scheduling considering electric energy and reserve markets. *AICHE J*. 2015;61(5):1547-1558.
55. Beal L, Petersen D, Pila G, Davis B, Warnick S, Hedengren JD. Eco nomic benefit from progressive integration of scheduling and control for continuous chemical processes. *PRO*. 2017;5(4):84.
56. Baader FJ, Althaus P, Bardow A, Dahmen M. Dynamic ramping for demand response of processes and energy systems based on exact linearization. *J Process Control*. 2022;118:218-230.
57. Zhuge J, Ierapetritou MG. A decomposition approach for the solution of scheduling including process dynamics of continuous processes. *Ind Eng Chem Res*. 2016;55(5):1266-1280.
58. Kadam J, Marquardt W, Schlegel M, et al. Towards integrated dynamic real-time optimization and control of industrial processes. *Proceedings Foundations of Computer-Aided Process Operations (FOCAPO2003)*. Computer Aids for Chemical Engineering; 2003:593-596.
59. Nyström RH, Franke R, Harjunkoski I, Kroll A. Production campaign planning including grade transition sequencing and dynamic optimization. *Comput Chem Eng*. 2005;29(10):2163-2179.
60. Zhuge J, Ierapetritou MG. Integration of scheduling and control with closed loop implementation. *Ind Eng Chem Res*. 2012;51(25):8550-8565.
61. Semrau R, Engell S. Process as a battery: Electricity price aware optimal operation of zeolite crystallization in a continuous oscillatory baffled reactor. *Comput Chem Eng*. 2023;171:108143.
62. Zhuge J, Ierapetritou MG. An integrated framework for scheduling and control using fast model predictive control. *AICHE J*. 2015;61(10):3304-3319.

63. Zhuge J, Ierapetritou MG. Integration of scheduling and control for batch processes using multi-parametric model predictive control. *AICHE J*. 2014;60(9):3169-3183.
64. Li H, Swartz CLE. Approximation techniques for dynamic real-time optimization (DRTO) of distributed MPC systems. *Comput Chem Eng*. 2018;118(1):195-209.
65. Kumar P, Rawlings JB, Carrette P. Modeling proportional-integral controllers in tracking and economic model predictive control. *J Process Control*. 2023;122:1-12.
66. Jamaludin MZ, Swartz CLE. Dynamic real-time optimization with closed-loop prediction. *AICHE J*. 2017;63(9):3896-3911.
67. Dering D, Swartz CLE. Dynamic real-time optimization with closed-loop prediction for nonlinear MPC-controlled plants. *32nd European Symposium on Computer Aided Process Engineering*. Computer Aided Chemical Engineering. Vol 51. Elsevier; 2022:1099-1104.
68. Burnak B, Katz J, Diangelakis NA, Pistikopoulos EN. Simultaneous process scheduling and control: A multiparametric programming-based approach. *Ind Eng Chem Res*. 2018;57(11):3963-3976.
69. Juan D, Park J, Harjunkoski I, Baldea M. A time scale-bridging approach for integrating production scheduling and process control. *Comput Chem Eng*. 2015;79:59-69.
70. Tsay C, Kumar A, Flores-Cerrillo J, Baldea M. Optimal demand response scheduling of an industrial air separation unit using data-driven dynamic models. *Comput Chem Eng*. 2019;126(1-2):22-34.
71. Kelley MT, Tsay C, Cao Y, Wang Y, Flores-Cerrillo J, Baldea M. A data-driven linear formulation of the optimal demand response scheduling problem for an industrial air separation unit. *Chem Eng Sci*. 2022;252(5):117468.
72. Swartz CLE, Kawajiri Y. Design for dynamic operation-A review and new perspectives for an increasingly dynamic plant operating environment. *Comput Chem Eng*. 2019;128:329-339.
73. Dias LS, Pattison RC, Tsay C, Baldea M, Ierapetritou MG. A simulation-based optimization framework for integrating scheduling and model predictive control, and its application to air separation units. *Comput Chem Eng*. 2018;113:139-151.
74. Kelley MT, Pattison RC, Baldick R, Baldea M. An MILP framework for optimizing demand response operation of air separation units. *Appl Energy*. 2018;222:951-966.
75. Tsay C, Baldea M. 110th anniversary: Using data to bridge the time and length scales of process systems. *Ind Eng Chem Res*. 2019;58(36):16696-16708.
76. Kappatou CD, Bongartz D, Najman J, Sass S, Mitsos A. Global dynamic optimization with Hammerstein-wiener models embedded. *J Global Optim*. 2022;84(2):321-347.
77. Papadimitriou C, Varelmann T, Schröder C, Jupke A, Mitsos A. Globally optimal scheduling of an electrochemical process via data-driven dynamic modeling and wavelet based adaptive grid refinement. *Optim Eng*. 2023;25(3):1719-1752.
78. Shengnan Zhao M, Ochoa P, Tang L, Lotero I, Gopalakrishnan A, Grossmann IE. Novel formulation for optimal schedule with demand side management in multiproduct air separation processes. *Ind Eng Chem Res*. 2019;58(8):3104-3117.
79. Baldea M, Juan D, Park J, Harjunkoski I. Integrated production scheduling and model predictive control of continuous processes. *AICHE J*. 2015;61(12):4179-4190.
80. Jäschke J, Skogestad S. NCO tracking and self-optimizing control in the context of realtime optimization. *J Process Control*. 2011;21(10):1407-1416.
81. Papadimitriou C, Schulze JC, Mitsos A. Representative electricity price profiles for European day-ahead and intraday spot markets. *arXiv preprint arXiv:2405.14403* 2024.
82. Caspari A, Faust JMM, Schäfer P, Mhamdi A, Mitsos A. Economic nonlinear model predictive control for flexible operation of air separation units. *IFAC-PapersOnLine*. 2018;51(20):295-300.
83. Hannemann R, Marquardt W, Naumann U, Gendler B. Discrete first- and second order adjoints and automatic differentiation for the sensitivity analysis of dynamic models. *Proc Comput Sci*. 2010;1(1):297-305.
84. Gill PE, Murray W, Saunders MA. SNOPT: An SQP algorithm for large-scale constrained optimization. *SIAM Rev*. 2005;47(1):99-131.
85. EPEX. https://www.epexspot.com. Accessed: 2023-10-02. 2023.
86. Schäfer P, Daun TM, Mitsos A. Do investments in flexibility enhance sustain ability? A simulative study considering the German electricity sector. *AICHE J*. 2020;66:11.
87. Panagiotelis A, Smith M. Bayesian density forecasting of intraday electricity prices using multivariate skew t distributions. *Int J Forecast*. 2008). Energy Forecasting;24(4):710-727.
88. Cramer E, Witthaut D, Mitsos A, Dahmen M. Multivariate probabilistic forecasting of intraday electricity prices using normalizing flows. *Appl Energy*. 2023;346:121370.

SUPPORTING INFORMATION

Additional supporting information can be found online in the Supporting Information section at the end of this article.

How to cite this article: Schulze JC, Papadimitriou C, Kolmer P, Mitsos A. An integrated scheduling and control scheme with two economic layers for demand side management of chemical processes. *AIChE J*. 2025;e18731. doi:10.1002/aic.18731